Monthly Notices
of the
ROYAL ASTRONOMICAL SOCIETY

MNRAS **448,** 2749–2765 (2015) doi:10.1093/mnras/stv189

Determination of the spectroscopic stellar parameters for 257 field giant stars⋆

S. Alves,[1,2†] L. Benamati,[3,4,5] N. C. Santos,[3,4,5] V. Zh. Adibekyan,[3,4]
S. G. Sousa,[3,4,5] G. Israelian,[6,7] J. R. De Medeiros,[8] C. Lovis[9] and S. Udry[9]

[1]*Instituto de Astrofísica, Pontificia Universidad Católica de Chile, Av. Vicuña Mackenna 4860, 782-0436 Macul, Santiago, Chile*
[2]*CAPES Foundation, Ministry of Education of Brazil, 70040-020, Brasília / DF, Brazil*
[3]*Centro de Astrofísica da Universidade do Porto, Rua das Estrelas, P-4150-762 Porto, Portugal*
[4]*Instituto de Astrofísica e Ciências do Espaço, Universidade do Porto, Rua das Estrelas, P-4150-762 Porto, Portugal*
[5]*Departamento de Física e Astronomia, Faculdade de Ciências da Universidade do Porto, P-4150-762 Porto, Portugal*
[6]*Instituto de Astrofísica de Canarias, E-38200 La Laguna, Tenerife, Spain*
[7]*Departamento de Astrofísica, Universidad de La Laguna, E-38206 La Laguna, Tenerife, Spain*
[8]*Departamento de Física Teórica e Experimental, Universidade Federal do Rio Grande do Norte, Campus Universitário Lagoa Nova, 59072-970 Natal, RN, Brasil*
[9]*Observatoire de Genève, Université de Genève, 51 ch. des Maillettes, CH-1290 Sauverny, Switzerland*

Accepted 2015 January 26. Received 2015 January 20; in original form 2014 November 26

ABSTRACT

The study of stellar parameters of planet-hosting stars, such as metallicity and chemical abundances, help us to understand the theory of planet formation and stellar evolution. Here, we present a catalogue of accurate stellar atmospheric parameters and iron abundances for a sample of 257 K and G field evolved stars that are being surveyed for planets using precise radial-velocity measurements as part of the Coralie programme to search for planets around giants. The analysis was done using a set of high-resolution and high-signal-to-noise Ultraviolet and Visible Echelle Spectrograph spectra. The stellar parameters were derived using Fe I and II ionization and excitation equilibrium methods. To take into account possible effects related to the choice of the lines on the derived parameters, we used three different iron line-list sets in our analysis, and the results differ among themselves by a small factor for most of stars. For those stars with previous literature parameter estimates, we found very good agreement with our own values. In the present catalogue, we are providing new precise spectroscopic measurements of effective temperature, surface gravity, microturbulence, and metallicity for 190 stars for which it has not been found or published in previous articles.

Key words: methods: observational – techniques: spectroscopic – catalogues – stars: fundamental parameters – stars: late-type.

1 INTRODUCTION

Stellar mass and metallicity are the two main parameters that have been suggested to influence the planet formation process. To date, over 1800 extrasolar planets have been discovered and this number continues to increase. However, more than 90 per cent of these planets orbit main-sequence stars with masses smaller than 1.50 $M_{\odot}$. Because of this, our understanding of planet formation as a function of the mass of the host star, and of the stellar environments is poorly understood. Precise spectroscopic studies of field dwarf stars have suggested that the frequency of giant planets is a strong function of the stellar metallicity. It seems easier to find a planet around a metal-rich star than around a metal-poor object (e.g. Santos, Israelian & Mayor 2004; Fischer & Valenti 2005; Sousa et al. 2011). This result has usually been interpreted as due to a higher probability of forming a giant planet in a metal-rich environment. Such conclusion perfectly fits the core-accretion model for giant planet formation (e.g. Ida & Lin 2004; Mordasini et al. 2012).

Although the giant planet–metallicity correlation is well establish, there are number of details still missing, and some results have cast doubts into this subject. For instance, it was proposed that the metallicity–giant planet correlation may not be present for intermediate-mass stars hosting giant planets (Pasquini et al. 2007). Although this conclusion is not unanimous (see Hekker & Meléndez 2007; Reffert et al. 2015), the question is now being debated (Ghezzi et al. 2010; Maldonado, Villaver & Eiroa 2013; Mortier et al. 2013a).

⋆ Based on observations collected at the Paranal Observatory, ESO (Chile) with the Ultra-violet and Visible Echelle Spectrograph (UVES) of the VLT, under programmes 085.C-0062 and 086.C-0098.

† E-mail: salves@astro.puc.cl

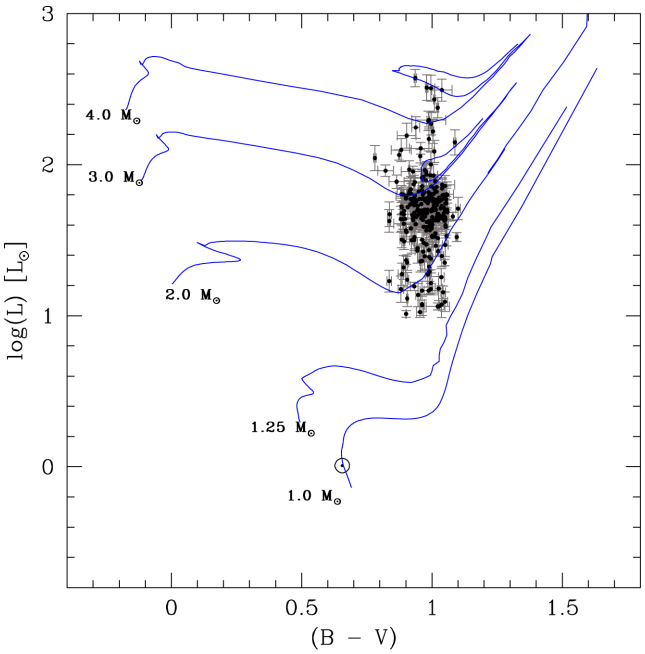

Figure 1. H–R diagram for our stellar sample. Evolutionary tracks from Ekström et al. (2012), for an initial abundance of metals set to $Z = 0.014$. The Sun is indicated by his usual symbol ⊙.

Indeed, in their recent work Reffert et al. (2015) argued that there are consistent indications for a planet–metallicity correlation among giant star planet hosts which matches the observed planet–metallicity correlation for main-sequence hosts, in sharp contrast with the results of Pasquini et al. (2007).

In fact, the discovery of several planets orbiting metal-poor objects (Cochran et al. 2007; Santos et al. 2008a,b) shows that giant planet formation is not completely inhibited in the metal-poor regime (see also discussion in Santos et al. 2004). This lends support to the idea that disc instability processes could also lead to the formation of giant planets (e.g. Boss 2002). It should also be noted that even though evolved planet hosts are on average more metal-poor than planet-hosting dwarfs,[1] there seems to be no metallicity enhancement present for red giants with planets regarding to red giants without planets detected (Mortier et al. 2013b, and references therein).

Concerning the intermediate-mass stars hosting planets, it could be, for example, that the higher mass of these stars, competing with the stellar metallicity, is changing the observed trends. If confirmed, however, the results of Pasquini et al. (2007) would cast doubts in the planet–metallicity relation observed for dwarf stars, or at least in the way this relation has been interpreted. These authors suggest that such a difference between main-sequence and evolved stars is due to pollution, which is more effective for stars in the main sequence than for evolved giant stars where the convective zone enlarge and mix a large fraction of the stellar gas. Other explanations are also possible: giants are on average more massive (see however Lloyd 2013) than main-sequence stars surveyed for planet search, therefore the frequency of planets around giants could be explained with more sophisticated models that take into account the dependence of the snow line with the stellar mass. It may produce a large increase of giant planets frequency with the stellar mass (Kennedy & Kenyon 2008). In this scheme, only the total amount of metals present (and not their percentage) is relevant, therefore more massive metal-poor stars (with more massive discs) may still produce many planets.

In fact, recent studies suggest that radial-velocity surveys of giant stars are biased with respect to metal-poor stars, once most of those programmes select their stellar samples with a cut-off in the $(B - V)$ colour, set to be less than or equal to 1.0. This $(B - V)$ cut-off in a sample of cool stars result in a lack of high-metallicity, low-gravity components, creating a bias that may explain why planets are rather found orbiting metal-poor giants (Mortier et al. 2013b). In addition, Santos et al. (2009) have shown that the derivation of the parameters should be considered as another explanation, since the way the lines are chosen may have a determining role for the derivation of metallicities for giant stars.

A clear answer to these questions is fundamental for our understanding of planet formation models. One way to approach this issue would be to explore the frequency of giant planets orbiting intermediate-mass stars. However, given the huge difficulties of obtaining precise radial velocities for massive main-sequence stars, one of the most effective ways to access the frequency of planets around higher mass stars is to search for planets around giants. Unfortunately, it is not easy to derive the mass for a highly evolved field star. Red giant phase, red giant branch and horizontal branch stars with different ages, masses, and metallicities occupy a similar position in the Hertzprung–Russel (H–R) diagram, the so called mass–age–metallicity degeneracy, and therefore the mass and evolutionary status cannot be determined simply by comparing their effective temperature and luminosity with isomass tracks (Jones et al. 2011).[2] Due to this it is more difficult to study the 'stellar mass–frequency of planets' relation for giant stars. A more accurate derivation of uniform and precise parameters for the giants in planet search samples is needed if we want to overcome this problem (Santos et al. 2009).

In this paper, we present a catalogue of accurate atmospheric parameters for a sample of 257 field giant stars that are being surveyed for planets using precise radial-velocity measurements. These results will be very useful to study the frequency of planets as a function of the different stellar parameters, including their chemical composition (Adibekyan et al., in preparation) and mass, and confront the results with model predictions. Also, homogeneous determination of parameters for comparison works are fundamental to avoid possible misconceptions, such as systematic deviations intrinsic to the use of different approaches for measuring atmospheric parameters.

This paper is arranged as follows. In Section 2, we present the stellar sample. In Section 3, we present the method used to derive the spectroscopic parameters, and the results obtained, discussing the implications of the use of different line-lists to derive the parameters. In Section 4, we compare our results with literature data. We conclude in Section 5.

2 STELLAR SAMPLE

For this analysis, we used a sample of 257 K and G evolved stars, that are being surveyed for planets using precise radial-velocity

[1] However, it should be considered the possibility that giant stellar samples that are searched for planets may are biased. Hence, the comparison of dwarf stars with giant stars should be done cautiously.

[2] Note that using asteroseismology the degenerency observed in the H–R diagram may be broken and then we can have better accuracy/precision for mass estimation.

Table 1. Stellar parameters determined from the iron lines by using HM07, SO08, and TS13 line-lists. The adopted parameters in our work is the one derived with the TS13 line-list.

	HM07 line-list				S08 line-list				T13 line-list			
HD number	$T_{\rm eff}$ (K)	log g (cm s^{-2})	ξ (km s^{-1})	[Fe/H] (dex)	$T_{\rm eff}$ (K)	log g (cm s^{-2})	ξ (km s^{-1})	[Fe/H] (dex)	$T_{\rm eff}$ (K)	log g (cm s^{-2})	ξ (km s^{-1})	[Fe/H] (dex)
496	4881 ± 225	2.78 ± 0.45	1.21 ± 0.20	0.05 ± 0.18	4900 ± 39	2.79 ± 0.07	1.52 ± 0.04	−0.03 ± 0.03	4854 ± 40	2.75 ± 0.10	1.46 ± 0.04	−0.03 ± 0.03
636	4784 ± 202	2.86 ± 0.41	1.26 ± 0.20	0.24 ± 0.31	4903 ± 46	2.87 ± 0.09	1.50 ± 0.04	0.13 ± 0.03	4840 ± 43	2.75 ± 0.11	1.46 ± 0.04	0.10 ± 0.03
770	4800 ± 208	2.66 ± 0.42	1.25 ± 0.20	−0.03 ± 0.32	4841 ± 35	2.59 ± 0.07	1.52 ± 0.03	−0.13 ± 0.03	4771 ± 45	2.47 ± 0.10	1.50 ± 0.04	−0.16 ± 0.03
1737	4797 ± 203	2.36 ± 0.42	1.25 ± 0.20	0.13 ± 0.51	4998 ± 47	2.75 ± 0.08	1.57 ± 0.05	0.13 ± 0.04	4932 ± 50	2.57 ± 0.12	1.54 ± 0.05	0.10 ± 0.04
3488	4869 ± 63	2.87 ± 0.11	1.56 ± 0.09	−0.08 ± 0.06	4935 ± 30	2.83 ± 0.06	1.50 ± 0.03	−0.08 ± 0.03	4880 ± 34	2.72 ± 0.08	1.44 ± 0.04	−0.10 ± 0.03
4737	5146 ± 61	3.09 ± 0.09	1.14 ± 0.09	0.05 ± 0.06	5217 ± 26	3.20 ± 0.07	1.35 ± 0.03	0.01 ± 0.02	5199 ± 30	3.03 ± 0.10	1.34 ± 0.03	0.00 ± 0.03
5457	4682 ± 90	2.85 ± 0.18	1.36 ± 0.10	−0.02 ± 0.07	4727 ± 44	2.78 ± 0.09	1.36 ± 0.04	−0.05 ± 0.03	4706 ± 46	2.78 ± 0.10	1.36 ± 0.05	−0.05 ± 0.03
6080	5034 ± 70	3.43 ± 0.11	1.18 ± 0.10	−0.08 ± 0.06	5118 ± 25	3.46 ± 0.04	1.12 ± 0.03	−0.07 ± 0.02	5084 ± 24	3.38 ± 0.05	1.14 ± 0.03	−0.09 ± 0.02
6192	4995 ± 102	2.87 ± 0.16	1.51 ± 0.14	−0.04 ± 0.10	5124 ± 32	3.05 ± 0.07	1.45 ± 0.03	0.04 ± 0.03	5122 ± 26	2.99 ± 0.11	1.42 ± 0.03	0.05 ± 0.02
6245	5115 ± 62	3.21 ± 0.09	1.25 ± 0.09	0.04 ± 0.06	5179 ± 23	3.16 ± 0.05	1.33 ± 0.03	0.02 ± 0.02	5163 ± 26	3.12 ± 0.07	1.28 ± 0.03	0.02 ± 0.03
6793[a]	5178 ± 74	3.15 ± 0.13	1.41 ± 0.13	−0.02 ± 0.08	5367 ± 33	3.49 ± 0.10	1.70 ± 0.04	0.03 ± 0.03	5330 ± 42	3.27 ± 0.11	1.55 ± 0.04	0.03 ± 0.04
7082	4979 ± 93	2.75 ± 0.09	1.75 ± 0.44	−0.76 ± 0.11	5047 ± 18	2.70 ± 0.04	1.70 ± 0.03	−0.75 ± 0.02	5048 ± 21	2.69 ± 0.09	1.67 ± 0.04	−0.74 ± 0.02
8651	4739 ± 203	2.61 ± 0.41	1.28 ± 0.20	−0.11 ± 0.06	4798 ± 37	2.64 ± 0.07	1.58 ± 0.03	−0.19 ± 0.03	4763 ± 42	2.66 ± 0.11	1.56 ± 0.04	−0.20 ± 0.03
9163	4865 ± 59	3.20 ± 0.11	1.13 ± 0.08	−0.12 ± 0.04	4930 ± 27	3.18 ± 0.05	1.16 ± 0.03	−0.14 ± 0.02	4898 ± 29	3.12 ± 0.07	1.14 ± 0.03	−0.15 ± 0.02
9362	4824 ± 66	2.59 ± 0.11	1.46 ± 0.11	−0.30 ± 0.07	4895 ± 26	2.64 ± 0.04	1.50 ± 0.03	−0.28 ± 0.02	4885 ± 32	2.60 ± 0.07	1.49 ± 0.03	−0.29 ± 0.03
9525	4764 ± 214	3.08 ± 0.43	1.27 ± 0.20	0.12 ± 0.50	4808 ± 48	2.88 ± 0.09	1.42 ± 0.05	0.00 ± 0.03	4725 ± 70	2.71 ± 0.16	1.33 ± 0.07	−0.02 ± 0.04
10142	4727 ± 67	2.57 ± 0.13	1.51 ± 0.08	−0.14 ± 0.05	4815 ± 45	2.61 ± 0.09	1.53 ± 0.05	−0.11 ± 0.04	4755 ± 34	2.47 ± 0.09	1.50 ± 0.04	−0.15 ± 0.03
11977	4968 ± 98	2.88 ± 0.16	1.62 ± 0.17	−0.19 ± 0.10	5054 ± 21	2.90 ± 0.04	1.46 ± 0.02	−0.15 ± 0.02	5018 ± 27	2.85 ± 0.07	1.44 ± 0.03	−0.17 ± 0.03
12055[a]	5118 ± 204	2.84 ± 0.41	1.09 ± 0.20	−0.04 ± 0.63	5265 ± 30	3.11 ± 0.07	1.54 ± 0.03	−0.02 ± 0.03	5255 ± 27	3.04 ± 0.15	1.45 ± 0.03	−0.02 ± 0.02
12296	4751 ± 57	2.76 ± 0.12	1.49 ± 0.07	0.01 ± 0.05	4811 ± 32	2.65 ± 0.06	1.53 ± 0.03	−0.04 ± 0.02	4787 ± 33	2.60 ± 0.09	1.51 ± 0.03	−0.05 ± 0.03
12431	4997 ± 71	2.90 ± 0.14	1.35 ± 0.10	0.04 ± 0.07	5049 ± 30	2.93 ± 0.06	1.43 ± 0.03	0.00 ± 0.02	5010 ± 36	2.83 ± 0.09	1.43 ± 0.04	−0.03 ± 0.03
12438	4956 ± 77	2.58 ± 0.09	1.70 ± 0.24	−0.62 ± 0.08	5050 ± 14	2.69 ± 0.04	1.64 ± 0.02	−0.57 ± 0.01	5056 ± 20	2.70 ± 0.04	1.66 ± 0.03	−0.57 ± 0.02
13263	5098 ± 67	3.06 ± 0.10	1.39 ± 0.12	−0.06 ± 0.07	5181 ± 21	3.09 ± 0.04	1.36 ± 0.02	−0.04 ± 0.02	5173 ± 25	3.08 ± 0.07	1.38 ± 0.03	−0.05 ± 0.02
13940	4996 ± 65	3.02 ± 0.11	1.35 ± 0.10	0.02 ± 0.06	5050 ± 25	2.99 ± 0.04	1.43 ± 0.03	0.00 ± 0.02	5017 ± 32	2.90 ± 0.07	1.43 ± 0.03	−0.02 ± 0.03
14247	4840 ± 55	3.12 ± 0.10	1.28 ± 0.07	−0.13 ± 0.05	4895 ± 28	3.05 ± 0.05	1.24 ± 0.03	−0.15 ± 0.02	4857 ± 33	2.97 ± 0.06	1.22 ± 0.03	−0.17 ± 0.03
14703	4966 ± 204	2.91 ± 0.42	1.17 ± 0.20	0.15 ± 0.43	5100 ± 25	3.13 ± 0.06	1.37 ± 0.03	0.12 ± 0.02	5058 ± 33	3.10 ± 0.10	1.38 ± 0.04	0.09 ± 0.03
14832	4826 ± 70	2.70 ± 0.13	1.50 ± 0.09	−0.23 ± 0.07	4890 ± 26	2.66 ± 0.05	1.50 ± 0.03	−0.23 ± 0.02	4862 ± 28	2.59 ± 0.06	1.48 ± 0.03	−0.25 ± 0.02
15414	4756 ± 60	3.21 ± 0.12	1.08 ± 0.07	−0.02 ± 0.04	4843 ± 34	3.23 ± 0.07	1.14 ± 0.04	−0.06 ± 0.02	4803 ± 39	3.21 ± 0.10	1.07 ± 0.05	−0.06 ± 0.03
16815	4739 ± 57	2.74 ± 0.11	1.33 ± 0.08	−0.32 ± 0.05	4794 ± 24	2.69 ± 0.06	1.35 ± 0.03	−0.34 ± 0.02	4777 ± 27	2.65 ± 0.10	1.33 ± 0.03	−0.34 ± 0.02
16975	5065 ± 201	2.88 ± 0.43	1.12 ± 0.20	0.15 ± 0.85	5162 ± 24	3.02 ± 0.04	1.41 ± 0.02	0.07 ± 0.02	5159 ± 25	3.05 ± 0.08	1.43 ± 0.03	0.07 ± 0.02
17324	4868 ± 68	3.15 ± 0.11	1.25 ± 0.10	−0.15 ± 0.05	4916 ± 27	3.11 ± 0.05	1.18 ± 0.03	−0.16 ± 0.02	4902 ± 30	3.05 ± 0.07	1.19 ± 0.03	−0.17 ± 0.02
17374	4881 ± 64	2.85 ± 0.11	1.37 ± 0.09	−0.02 ± 0.06	4923 ± 25	2.77 ± 0.04	1.47 ± 0.03	−0.08 ± 0.02	4899 ± 28	2.75 ± 0.06	1.45 ± 0.03	−0.09 ± 0.02
17504	4910 ± 57	3.20 ± 0.09	1.19 ± 0.09	−0.25 ± 0.05	4962 ± 21	3.18 ± 0.03	1.16 ± 0.02	−0.26 ± 0.02	4961 ± 24	3.18 ± 0.05	1.16 ± 0.03	−0.26 ± 0.02
17652	4820 ± 63	2.66 ± 0.10	1.51 ± 0.10	−0.30 ± 0.06	4868 ± 23	2.62 ± 0.05	1.51 ± 0.02	−0.32 ± 0.02	4872 ± 27	2.59 ± 0.06	1.51 ± 0.03	−0.32 ± 0.03
17715	4842 ± 56	2.67 ± 0.10	1.43 ± 0.07	−0.06 ± 0.05	4961 ± 33	2.83 ± 0.06	1.50 ± 0.03	−0.01 ± 0.03	4920 ± 31	2.69 ± 0.08	1.46 ± 0.03	−0.03 ± 0.03
18023	4686 ± 208	2.72 ± 0.42	1.31 ± 0.20	−0.30 ± 0.15	4770 ± 28	2.73 ± 0.07	1.29 ± 0.03	−0.28 ± 0.02	4740 ± 28	2.61 ± 0.12	1.28 ± 0.03	−0.31 ± 0.02
18121	4761 ± 63	2.62 ± 0.12	1.34 ± 0.08	−0.10 ± 0.06	4837 ± 37	2.65 ± 0.07	1.43 ± 0.04	−0.14 ± 0.03	4792 ± 43	2.54 ± 0.09	1.42 ± 0.04	−0.17 ± 0.03
18292	4818 ± 206	2.69 ± 0.41	1.24 ± 0.20	0.13 ± 0.40	5004 ± 34	2.94 ± 0.08	1.47 ± 0.04	0.13 ± 0.03	4930 ± 43	2.85 ± 0.10	1.45 ± 0.04	0.09 ± 0.03
18448	4724 ± 72	2.59 ± 0.13	1.50 ± 0.10	−0.31 ± 0.07	4791 ± 30	2.62 ± 0.08	1.60 ± 0.03	−0.33 ± 0.03	4756 ± 32	2.60 ± 0.09	1.54 ± 0.04	−0.34 ± 0.03
18650	4745 ± 206	2.62 ± 0.41	1.28 ± 0.20	0.15 ± 0.57	4912 ± 43	2.86 ± 0.08	1.47 ± 0.04	0.12 ± 0.03	4823 ± 35	2.65 ± 0.09	1.47 ± 0.04	0.06 ± 0.03
19940	4804 ± 218	2.95 ± 0.44	1.25 ± 0.20	−0.02 ± 0.56	4905 ± 38	2.97 ± 0.06	1.32 ± 0.04	−0.05 ± 0.03	4854 ± 41	2.90 ± 0.09	1.28 ± 0.04	−0.06 ± 0.03
21011	4885 ± 80	2.85 ± 0.13	1.39 ± 0.10	−0.04 ± 0.07	4972 ± 30	2.89 ± 0.05	1.47 ± 0.03	−0.06 ± 0.03	4934 ± 33	2.82 ± 0.07	1.46 ± 0.04	−0.09 ± 0.03
21430	4919 ± 72	2.61 ± 0.10	1.42 ± 0.14	−0.36 ± 0.07	4983 ± 18	2.67 ± 0.04	1.48 ± 0.02	−0.36 ± 0.02	4987 ± 21	2.66 ± 0.06	1.49 ± 0.03	−0.35 ± 0.02

Table 1. – *continued*

HD number	HM07 line-list $T_{\rm eff}$ (K)	HM07 line-list $\log g$ (cm s^{-2})	HM07 line-list ξ (km s^{-1})	HM07 line-list [Fe/H] (dex)	S08 line-list $T_{\rm eff}$ (K)	S08 line-list $\log g$ (cm s^{-2})	S08 line-list ξ (km s^{-1})	S08 line-list [Fe/H] (dex)	T13 line-list $T_{\rm eff}$ (K)	T13 line-list $\log g$ (cm s^{-2})	T13 line-list ξ (km s^{-1})	T13 line-list [Fe/H] (dex)
22366	4678 ± 65	2.68 ± 0.12	1.40 ± 0.08	−0.36 ± 0.05	4740 ± 22	2.67 ± 0.04	1.35 ± 0.02	−0.37 ± 0.02	4734 ± 27	2.68 ± 0.06	1.36 ± 0.03	−0.37 ± 0.02
22382	4809 ± 215	2.72 ± 0.43	1.25 ± 0.20	0.10 ± 0.53	4920 ± 35	2.90 ± 0.07	1.49 ± 0.03	0.07 ± 0.03	4851 ± 38	2.72 ± 0.09	1.51 ± 0.04	0.01 ± 0.03
22532	4996 ± 73	3.22 ± 0.12	1.16 ± 0.12	−0.20 ± 0.07	5061 ± 18	3.22 ± 0.04	1.19 ± 0.02	−0.22 ± 0.02	5047 ± 19	3.20 ± 0.06	1.19 ± 0.02	−0.22 ± 0.02
22676	5045 ± 309	3.01 ± 0.62	1.13 ± 0.20	0.12 ± 0.22	5147 ± 32	3.11 ± 0.08	1.47 ± 0.04	0.06 ± 0.03	5109 ± 36	3.01 ± 0.09	1.40 ± 0.04	0.06 ± 0.03
23549	4885 ± 204	2.88 ± 0.41	1.21 ± 0.20	0.27 ± 0.20	5038 ± 33	2.99 ± 0.07	1.51 ± 0.03	0.18 ± 0.03	4992 ± 39	2.96 ± 0.10	1.48 ± 0.04	0.16 ± 0.03
23670	4877 ± 215	2.71 ± 0.45	1.21 ± 0.20	−0.06 ± 0.24	4883 ± 27	2.68 ± 0.05	1.48 ± 0.03	−0.16 ± 0.02	4884 ± 30	2.68 ± 0.07	1.48 ± 0.03	−0.16 ± 0.03
23719	4945 ± 206	2.63 ± 0.44	1.18 ± 0.20	0.17 ± 0.14	5103 ± 34	2.95 ± 0.05	1.52 ± 0.03	0.13 ± 0.03	5061 ± 31	2.87 ± 0.08	1.50 ± 0.03	0.12 ± 0.03
23931	4811 ± 207	2.75 ± 0.42	1.25 ± 0.20	0.01 ± 0.32	4853 ± 35	2.73 ± 0.07	1.48 ± 0.04	−0.08 ± 0.03	4785 ± 33	2.63 ± 0.09	1.47 ± 0.03	−0.11 ± 0.03
23940	4795 ± 60	2.57 ± 0.10	1.49 ± 0.11	−0.38 ± 0.06	4917 ± 24	2.59 ± 0.13	1.56 ± 0.03	−0.33 ± 0.02	4939 ± 26	2.52 ± 0.30	1.57 ± 0.03	−0.34 ± 0.03
24160	5047 ± 61	2.78 ± 0.10	1.37 ± 0.10	0.08 ± 0.07	5153 ± 25	2.94 ± 0.06	1.52 ± 0.03	0.08 ± 0.02	5136 ± 26	2.85 ± 0.08	1.53 ± 0.03	0.08 ± 0.02
28093	4885 ± 63	2.52 ± 0.10	1.46 ± 0.10	−0.19 ± 0.07	5011 ± 28	2.69 ± 0.07	1.61 ± 0.03	−0.15 ± 0.03	4994 ± 28	2.60 ± 0.15	1.58 ± 0.03	−0.15 ± 0.03
28732	4889 ± 217	2.83 ± 0.44	1.21 ± 0.20	0.10 ± 0.33	4999 ± 35	2.98 ± 0.06	1.46 ± 0.03	0.08 ± 0.03	4928 ± 33	2.86 ± 0.08	1.44 ± 0.03	0.05 ± 0.03
29085	4842 ± 57	3.05 ± 0.10	1.27 ± 0.08	−0.18 ± 0.04	4910 ± 26	3.07 ± 0.05	1.25 ± 0.03	−0.18 ± 0.02	4879 ± 29	3.00 ± 0.06	1.22 ± 0.03	−0.19 ± 0.02
29291	5080 ± 207	2.70 ± 0.44	1.11 ± 0.20	0.19 ± 0.55	5070 ± 31	2.75 ± 0.05	1.64 ± 0.03	0.02 ± 0.03	5074 ± 30	2.77 ± 0.07	1.61 ± 0.03	0.04 ± 0.03
29399	4831 ± 219	3.39 ± 0.44	1.24 ± 0.20	0.12 ± 0.33	4914 ± 45	3.36 ± 0.09	1.27 ± 0.05	0.09 ± 0.03	4828 ± 53	3.27 ± 0.16	1.12 ± 0.07	0.11 ± 0.03
29751	5054 ± 80	2.91 ± 0.13	1.46 ± 0.14	−0.10 ± 0.08	5109 ± 21	2.87 ± 0.04	1.54 ± 0.02	−0.12 ± 0.02	5052 ± 21	2.75 ± 0.08	1.53 ± 0.02	−0.16 ± 0.02
29930	4656 ± 65	2.43 ± 0.13	1.51 ± 0.07	−0.04 ± 0.05	4823 ± 50	2.62 ± 0.10	1.52 ± 0.05	0.03 ± 0.03	4748 ± 58	2.47 ± 0.13	1.53 ± 0.06	−0.02 ± 0.04
30185	4901 ± 204	2.85 ± 0.41	1.20 ± 0.20	−0.04 ± 0.69	4960 ± 29	2.85 ± 0.05	1.42 ± 0.03	−0.09 ± 0.02	4905 ± 33	2.77 ± 0.09	1.40 ± 0.03	−0.13 ± 0.03
30790	4739 ± 63	2.60 ± 0.12	1.46 ± 0.08	−0.01 ± 0.06	4925 ± 48	2.86 ± 0.09	1.49 ± 0.05	0.07 ± 0.04	4817 ± 49	2.59 ± 0.12	1.48 ± 0.05	0.00 ± 0.04
32436	4697 ± 230	2.56 ± 0.46	1.30 ± 0.20	0.15 ± 0.34	4871 ± 39	2.82 ± 0.07	1.58 ± 0.04	0.10 ± 0.03	4773 ± 57	2.61 ± 0.13	1.56 ± 0.05	0.04 ± 0.04
32453	5176 ± 118	3.18 ± 0.14	1.38 ± 0.23	−0.02 ± 0.13	5186 ± 22	3.06 ± 0.04	1.45 ± 0.02	−0.06 ± 0.02	5171 ± 27	2.99 ± 0.06	1.43 ± 0.03	−0.06 ± 0.03
33285	4902 ± 87	2.31 ± 0.15	1.87 ± 0.14	−0.09 ± 0.09	5133 ± 39	2.68 ± 0.07	2.09 ± 0.05	0.01 ± 0.04	5088 ± 44	2.54 ± 0.11	1.92 ± 0.05	0.00 ± 0.04
34172	5111 ± 211	3.04 ± 0.42	1.09 ± 0.20	0.13 ± 0.93	5156 ± 30	3.06 ± 0.05	1.44 ± 0.03	0.05 ± 0.03	5140 ± 35	3.02 ± 0.10	1.38 ± 0.04	0.06 ± 0.03
34266	4929 ± 218	2.61 ± 0.44	1.19 ± 0.20	0.10 ± 0.33	4975 ± 31	2.66 ± 0.06	1.63 ± 0.03	0.01 ± 0.03	4978 ± 34	2.70 ± 0.08	1.64 ± 0.04	0.01 ± 0.03
34642	4857 ± 401	3.34 ± 0.80	1.22 ± 0.20	−0.01 ± 0.85	4895 ± 29	3.20 ± 0.05	1.17 ± 0.04	−0.06 ± 0.02	4865 ± 30	3.16 ± 0.06	1.13 ± 0.04	−0.06 ± 0.02
36189	4913 ± 74	2.35 ± 0.12	1.80 ± 0.14	−0.12 ± 0.09	5068 ± 32	2.43 ± 0.12	1.92 ± 0.04	−0.05 ± 0.03	5053 ± 39	2.50 ± 0.10	1.83 ± 0.05	−0.05 ± 0.04
37811	5067 ± 67	2.87 ± 0.10	1.52 ± 0.11	−0.01 ± 0.07	5178 ± 22	2.94 ± 0.05	1.55 ± 0.02	0.02 ± 0.02	5136 ± 28	2.88 ± 0.07	1.52 ± 0.03	−0.01 ± 0.03
39640	4904 ± 56	2.81 ± 0.09	1.44 ± 0.08	−0.08 ± 0.06	4992 ± 33	2.84 ± 0.06	1.48 ± 0.04	−0.08 ± 0.03	4932 ± 36	2.70 ± 0.08	1.43 ± 0.04	−0.11 ± 0.03
39720	4727 ± 53	2.57 ± 0.10	1.59 ± 0.07	−0.19 ± 0.05	4790 ± 34	2.51 ± 0.07	1.56 ± 0.03	−0.19 ± 0.03	4770 ± 39	2.45 ± 0.09	1.53 ± 0.04	−0.19 ± 0.03
40409	4789 ± 201	3.31 ± 0.40	1.26 ± 0.20	0.10 ± 0.96	4838 ± 44	3.14 ± 0.09	1.20 ± 0.04	0.08 ± 0.03	4806 ± 48	3.14 ± 0.11	1.17 ± 0.06	0.08 ± 0.03
41451	4849 ± 201	2.77 ± 0.40	1.23 ± 0.20	0.28 ± 0.99	4966 ± 42	2.85 ± 0.09	1.54 ± 0.05	0.16 ± 0.04	4893 ± 58	2.78 ± 0.15	1.45 ± 0.06	0.17 ± 0.04
44880	4946 ± 205	3.05 ± 0.41	1.18 ± 0.20	−0.21 ± 0.69	5050 ± 21	3.20 ± 0.04	1.22 ± 0.02	−0.19 ± 0.02	5036 ± 22	3.14 ± 0.04	1.23 ± 0.03	−0.21 ± 0.02
44956	5102 ± 204	3.07 ± 0.43	1.10 ± 0.20	−0.02 ± 0.69	5219 ± 23	3.27 ± 0.05	1.39 ± 0.03	−0.03 ± 0.02	5163 ± 21	3.13 ± 0.09	1.33 ± 0.02	−0.05 ± 0.02
45145	4831 ± 57	2.82 ± 0.11	1.50 ± 0.07	0.00 ± 0.05	4935 ± 30	2.78 ± 0.10	1.54 ± 0.03	−0.01 ± 0.03	4891 ± 35	2.58 ± 0.21	1.49 ± 0.03	−0.04 ± 0.03
45158	5009 ± 201	3.08 ± 0.40	1.15 ± 0.20	0.18 ± 0.91	5091 ± 27	3.05 ± 0.06	1.36 ± 0.03	0.10 ± 0.02	5062 ± 39	2.99 ± 0.08	1.35 ± 0.04	0.07 ± 0.03
45553	5103 ± 74	3.14 ± 0.12	1.27 ± 0.11	0.06 ± 0.07	5184 ± 28	3.13 ± 0.05	1.37 ± 0.03	0.05 ± 0.03	5168 ± 33	3.07 ± 0.10	1.34 ± 0.04	0.05 ± 0.03
46116	4854 ± 57	2.65 ± 0.09	1.57 ± 0.10	−0.33 ± 0.06	4917 ± 25	2.70 ± 0.04	1.51 ± 0.03	−0.30 ± 0.02	4903 ± 26	2.63 ± 0.07	1.51 ± 0.03	−0.32 ± 0.02
46262	4693 ± 212	2.96 ± 0.42	1.31 ± 0.20	−0.32 ± 0.06	4746 ± 27	2.89 ± 0.06	1.26 ± 0.03	−0.34 ± 0.02	4716 ± 29	2.90 ± 0.07	1.21 ± 0.03	−0.34 ± 0.02
46727	4901 ± 60	2.84 ± 0.10	1.45 ± 0.09	−0.05 ± 0.06	4942 ± 31	2.75 ± 0.05	1.47 ± 0.04	−0.09 ± 0.03	4922 ± 41	2.73 ± 0.08	1.46 ± 0.05	−0.10 ± 0.03
47001	4681 ± 72	2.46 ± 0.13	1.53 ± 0.10	−0.25 ± 0.07	4724 ± 29	2.39 ± 0.08	1.61 ± 0.03	−0.32 ± 0.02	4703 ± 31	2.24 ± 0.12	1.57 ± 0.03	−0.33 ± 0.03
47910	4814 ± 70	2.75 ± 0.13	1.32 ± 0.08	−0.02 ± 0.06	4922 ± 31	2.82 ± 0.06	1.45 ± 0.03	−0.05 ± 0.03	4844 ± 33	2.65 ± 0.08	1.40 ± 0.03	−0.09 ± 0.03
47973	5062 ± 210	2.68 ± 0.46	1.12 ± 0.20	0.25 ± 0.67	5071 ± 46	2.67 ± 0.10	1.75 ± 0.06	0.06 ± 0.04	5048 ± 59	2.73 ± 0.11	1.68 ± 0.07	0.06 ± 0.05
48758	4785 ± 64	2.86 ± 0.11	1.30 ± 0.13	−0.59 ± 0.06	4871 ± 18	2.93 ± 0.03	1.27 ± 0.02	−0.57 ± 0.02	4864 ± 22	2.95 ± 0.04	1.28 ± 0.03	−0.57 ± 0.02
49947	4910 ± 221	2.63 ± 0.44	1.20 ± 0.20	−0.18 ± 0.36	5002 ± 23	2.87 ± 0.05	1.47 ± 0.03	−0.19 ± 0.02	4984 ± 28	2.80 ± 0.06	1.49 ± 0.04	−0.20 ± 0.02

Table 1. – *continued*

HD number	HM07 line-list $T_{\rm eff}$ (K)	HM07 line-list log g (cm s^{-2})	HM07 line-list ξ (km s^{-1})	HM07 line-list [Fe/H] (dex)	S08 line-list $T_{\rm eff}$ (K)	S08 line-list log g (cm s^{-2})	S08 line-list ξ (km s^{-1})	S08 line-list [Fe/H] (dex)	T13 line-list $T_{\rm eff}$ (K)	T13 line-list log g (cm s^{-2})	T13 line-list ξ (km s^{-1})	T13 line-list [Fe/H] (dex)
51211	4860 ± 71	2.79 ± 0.13	1.41 ± 0.10	−0.12 ± 0.07	4927 ± 26	2.73 ± 0.05	1.50 ± 0.03	−0.16 ± 0.02	4899 ± 27	2.70 ± 0.08	1.47 ± 0.03	−0.16 ± 0.02
55151	4792 ± 62	2.77 ± 0.14	1.52 ± 0.08	−0.02 ± 0.05	4873 ± 30	2.83 ± 0.08	1.51 ± 0.03	0.01 ± 0.03	4814 ± 36	2.79 ± 0.15	1.46 ± 0.04	−0.01 ± 0.02
55865	4817 ± 60	2.82 ± 0.12	1.51 ± 0.08	0.00 ± 0.05	4926 ± 38	2.83 ± 0.07	1.50 ± 0.04	0.03 ± 0.03	4866 ± 34	2.70 ± 0.10	1.47 ± 0.04	−0.01 ± 0.03
55964	4901 ± 63	3.08 ± 0.11	1.26 ± 0.09	−0.10 ± 0.05	4972 ± 24	3.10 ± 0.04	1.30 ± 0.03	−0.11 ± 0.02	4941 ± 27	3.00 ± 0.07	1.26 ± 0.03	−0.12 ± 0.02
56478	4827 ± 56	2.73 ± 0.11	1.50 ± 0.08	−0.10 ± 0.05	4932 ± 31	2.77 ± 0.06	1.57 ± 0.03	−0.12 ± 0.03	4897 ± 34	2.68 ± 0.08	1.56 ± 0.04	−0.15 ± 0.03
58540	4750 ± 291	3.23 ± 0.58	1.28 ± 0.20	−0.02 ± 0.39	4782 ± 35	3.06 ± 0.07	1.18 ± 0.04	−0.06 ± 0.02	4732 ± 42	2.96 ± 0.10	1.12 ± 0.04	−0.07 ± 0.03
59219	4784 ± 104	2.32 ± 0.21	1.96 ± 0.16	−0.09 ± 0.10	5099 ± 67	3.00 ± 0.13	2.27 ± 0.10	0.06 ± 0.06	5081 ± 63	2.92 ± 0.20	2.14 ± 0.08	0.06 ± 0.05
59894	4920 ± 72	2.81 ± 0.12	1.36 ± 0.10	−0.12 ± 0.07	5012 ± 25	2.92 ± 0.04	1.46 ± 0.03	−0.12 ± 0.02	4996 ± 25	2.87 ± 0.06	1.45 ± 0.03	−0.13 ± 0.02
60060	4887 ± 351	2.86 ± 0.70	1.21 ± 0.20	0.07 ± 0.24	4900 ± 35	2.79 ± 0.06	1.50 ± 0.03	−0.07 ± 0.03	4882 ± 37	2.72 ± 0.08	1.46 ± 0.04	−0.08 ± 0.03
60574	4938 ± 72	2.62 ± 0.10	1.50 ± 0.15	−0.42 ± 0.08	5046 ± 18	2.82 ± 0.04	1.64 ± 0.02	−0.41 ± 0.02	5036 ± 24	2.78 ± 0.05	1.61 ± 0.03	−0.40 ± 0.02
60666	4752 ± 71	2.59 ± 0.13	1.35 ± 0.08	−0.07 ± 0.06	4886 ± 40	2.76 ± 0.07	1.47 ± 0.04	−0.05 ± 0.03	4784 ± 38	2.63 ± 0.11	1.45 ± 0.04	−0.10 ± 0.03
61642	4817 ± 59	2.69 ± 0.11	1.31 ± 0.07	−0.07 ± 0.05	4925 ± 35	2.79 ± 0.07	1.41 ± 0.04	−0.07 ± 0.03	4868 ± 41	2.65 ± 0.10	1.38 ± 0.04	−0.11 ± 0.03
61904	5046 ± 201	2.93 ± 0.40	1.13 ± 0.20	0.19 ± 0.82	5148 ± 26	3.07 ± 0.06	1.43 ± 0.03	0.11 ± 0.02	5102 ± 28	2.92 ± 0.10	1.41 ± 0.03	0.08 ± 0.03
62034	4850 ± 296	2.81 ± 0.59	1.23 ± 0.20	0.07 ± 0.32	4870 ± 33	2.73 ± 0.06	1.48 ± 0.03	−0.05 ± 0.03	4836 ± 32	2.68 ± 0.07	1.47 ± 0.03	−0.07 ± 0.02
62412	4900 ± 204	2.74 ± 0.41	1.20 ± 0.20	0.12 ± 0.43	5030 ± 36	2.90 ± 0.07	1.48 ± 0.04	0.06 ± 0.03	4966 ± 40	2.76 ± 0.09	1.45 ± 0.04	0.03 ± 0.03
62943	5042 ± 201	3.02 ± 0.41	1.13 ± 0.20	0.08 ± 0.82	5141 ± 23	3.11 ± 0.04	1.36 ± 0.02	0.03 ± 0.02	5114 ± 21	3.02 ± 0.10	1.35 ± 0.02	0.01 ± 0.02
63295	4721 ± 57	2.43 ± 0.10	1.41 ± 0.07	−0.18 ± 0.05	4896 ± 39	2.73 ± 0.06	1.48 ± 0.04	−0.10 ± 0.03	4837 ± 44	2.57 ± 0.09	1.44 ± 0.05	−0.13 ± 0.03
63744	4760 ± 67	2.78 ± 0.14	1.54 ± 0.09	−0.04 ± 0.05	4903 ± 57	2.86 ± 0.10	1.54 ± 0.06	0.00 ± 0.04	4815 ± 51	2.66 ± 0.12	1.41 ± 0.06	−0.02 ± 0.04
63948	4902 ± 60	3.03 ± 0.10	1.26 ± 0.09	−0.08 ± 0.06	5005 ± 26	3.10 ± 0.05	1.32 ± 0.03	−0.08 ± 0.02	4960 ± 26	3.02 ± 0.06	1.30 ± 0.03	−0.10 ± 0.02
64121	5018 ± 70	3.28 ± 0.12	1.19 ± 0.12	−0.24 ± 0.07	5077 ± 20	3.30 ± 0.04	1.18 ± 0.02	−0.25 ± 0.02	5072 ± 17	3.32 ± 0.05	1.18 ± 0.02	−0.25 ± 0.01
65638	4950 ± 49	2.93 ± 0.08	1.50 ± 0.08	0.02 ± 0.05	5015 ± 30	2.89 ± 0.05	1.44 ± 0.03	0.05 ± 0.03	4972 ± 30	2.81 ± 0.07	1.45 ± 0.03	0.02 ± 0.03
67762	4938 ± 204	3.44 ± 0.41	1.18 ± 0.20	−0.01 ± 0.49	5010 ± 28	3.42 ± 0.06	1.10 ± 0.03	−0.01 ± 0.02	4972 ± 30	3.36 ± 0.06	1.09 ± 0.04	−0.04 ± 0.02
67977	5057 ± 68	2.92 ± 0.08	1.37 ± 0.13	−0.18 ± 0.07	5165 ± 19	3.09 ± 0.04	1.40 ± 0.02	−0.13 ± 0.02	5142 ± 22	3.07 ± 0.06	1.41 ± 0.03	−0.15 ± 0.02
67990	4905 ± 63	2.90 ± 0.12	1.44 ± 0.08	−0.02 ± 0.06	5012 ± 30	2.92 ± 0.06	1.46 ± 0.03	0.00 ± 0.03	4925 ± 33	2.73 ± 0.09	1.40 ± 0.03	−0.05 ± 0.03
69123	4844 ± 56	3.13 ± 0.11	1.33 ± 0.07	0.07 ± 0.04	4885 ± 34	3.01 ± 0.07	1.35 ± 0.04	0.02 ± 0.03	4850 ± 40	2.81 ± 0.18	1.32 ± 0.04	−0.01 ± 0.03
69674	4789 ± 67	2.43 ± 0.11	1.55 ± 0.09	−0.20 ± 0.06	4888 ± 27	2.53 ± 0.05	1.59 ± 0.03	−0.17 ± 0.03	4871 ± 38	2.59 ± 0.08	1.62 ± 0.04	−0.19 ± 0.03
69879	4768 ± 53	2.64 ± 0.10	1.41 ± 0.07	−0.01 ± 0.04	4867 ± 36	2.71 ± 0.08	1.47 ± 0.03	−0.01 ± 0.03	4811 ± 35	2.63 ± 0.10	1.49 ± 0.04	−0.06 ± 0.03
70982	5037 ± 72	2.86 ± 0.12	1.43 ± 0.10	0.00 ± 0.07	5132 ± 27	2.89 ± 0.05	1.50 ± 0.03	0.02 ± 0.03	5132 ± 30	2.78 ± 0.13	1.45 ± 0.03	0.02 ± 0.03
73468	5000 ± 251	2.77 ± 0.50	1.15 ± 0.20	−0.06 ± 0.10	5036 ± 21	2.89 ± 0.04	1.48 ± 0.02	−0.13 ± 0.02	5012 ± 22	2.85 ± 0.07	1.46 ± 0.03	−0.14 ± 0.02
73887	4824 ± 54	2.73 ± 0.10	1.37 ± 0.07	0.04 ± 0.05	4927 ± 38	2.80 ± 0.07	1.51 ± 0.04	0.01 ± 0.03	4828 ± 43	2.60 ± 0.09	1.48 ± 0.04	−0.05 ± 0.04
73898	4958 ± 75	2.66 ± 0.10	1.60 ± 0.16	−0.48 ± 0.08	5034 ± 16	2.70 ± 0.04	1.53 ± 0.02	−0.44 ± 0.02	5055 ± 21	2.72 ± 0.06	1.54 ± 0.03	−0.43 ± 0.02
74006					5766 ± 149	3.92 ± 0.15	4.28 ± 0.42	−0.02 ± 0.12	5590 ± 168	3.73 ± 0.27	3.17 ± 0.49	−0.06 ± 0.13
74772[a]	5131 ± 128	2.67 ± 0.15	1.22 ± 0.27	−0.09 ± 0.12	5290 ± 24	2.93 ± 0.07	1.62 ± 0.03	−0.07 ± 0.02	5291 ± 32	2.89 ± 0.11	1.54 ± 0.04	−0.04 ± 0.03
75168[a]	5243 ± 80	2.99 ± 0.12	1.45 ± 0.16	−0.05 ± 0.09	5450 ± 27	3.23 ± 0.07	1.56 ± 0.03	0.06 ± 0.03	5444 ± 35	3.19 ± 0.14	1.52 ± 0.04	0.05 ± 0.03
75451	4819 ± 74	3.08 ± 0.14	1.18 ± 0.09	0.00 ± 0.05	4916 ± 31	3.12 ± 0.06	1.24 ± 0.04	−0.03 ± 0.03	4875 ± 31	3.04 ± 0.07	1.21 ± 0.03	−0.04 ± 0.02
77580	4850 ± 457	2.74 ± 0.92	1.23 ± 0.20	0.19 ± 0.06	5042 ± 43	3.01 ± 0.09	1.52 ± 0.04	0.16 ± 0.04	4991 ± 50	2.95 ± 0.10	1.46 ± 0.05	0.16 ± 0.04
78883	4840 ± 58	2.67 ± 0.09	1.65 ± 0.14	−0.52 ± 0.06	4994 ± 29	2.89 ± 0.07	1.69 ± 0.04	−0.42 ± 0.03	4984 ± 27	2.82 ± 0.12	1.59 ± 0.04	−0.42 ± 0.03
79091	4708 ± 59	2.94 ± 0.13	1.27 ± 0.07	−0.17 ± 0.04	4765 ± 26	2.86 ± 0.06	1.26 ± 0.03	−0.21 ± 0.02	4726 ± 33	2.80 ± 0.08	1.23 ± 0.04	−0.22 ± 0.02
79846	4983 ± 137	2.67 ± 0.30	2.55 ± 0.40	−0.13 ± 0.15	5300 ± 60	2.88 ± 0.15	2.43 ± 0.08	0.13 ± 0.06	5117 ± 75	2.77 ± 0.21	2.32 ± 0.11	0.00 ± 0.07
80171	4933 ± 202	2.94 ± 0.41	1.18 ± 0.20	0.22 ± 0.60	5034 ± 33	3.02 ± 0.08	1.48 ± 0.04	0.11 ± 0.03	5006 ± 47	2.97 ± 0.11	1.41 ± 0.05	0.12 ± 0.04
80934	4921 ± 201	3.04 ± 0.40	1.19 ± 0.20	0.22 ± 0.60	5042 ± 33	3.08 ± 0.07	1.42 ± 0.04	0.15 ± 0.03	5002 ± 46	3.03 ± 0.12	1.41 ± 0.05	0.13 ± 0.04
81101	4898 ± 79	2.65 ± 0.11	1.52 ± 0.15	−0.38 ± 0.08	4979 ± 19	2.75 ± 0.03	1.53 ± 0.02	−0.35 ± 0.02	4977 ± 24	2.72 ± 0.05	1.51 ± 0.03	−0.36 ± 0.02
81136[a]	5141 ± 74	2.90 ± 0.10	1.60 ± 0.13	0.07 ± 0.08	5222 ± 26	2.81 ± 0.07	1.68 ± 0.03	0.07 ± 0.02	5206 ± 30	2.78 ± 0.11	1.60 ± 0.03	0.08 ± 0.03
81169	5072 ± 217	2.95 ± 0.43	1.11 ± 0.20	−0.01 ± 0.15	5131 ± 22	3.06 ± 0.04	1.38 ± 0.02	−0.05 ± 0.02	5126 ± 22	3.04 ± 0.06	1.36 ± 0.03	−0.05 ± 0.02

Table 1. – *continued*

HD number	HM07 line-list $T_{\rm eff}$ (K)	HM07 line-list log g (cm s^{-2})	HM07 line-list ξ (km s^{-1})	HM07 line-list [Fe/H] (dex)	S08 line-list $T_{\rm eff}$ (K)	S08 line-list log g (cm s^{-2})	S08 line-list ξ (km s^{-1})	S08 line-list [Fe/H] (dex)	T13 line-list $T_{\rm eff}$ (K)	T13 line-list log g (cm s^{-2})	T13 line-list ξ (km s^{-1})	T13 line-list [Fe/H] (dex)
83380	4793 ± 202	2.74 ± 0.41	1.26 ± 0.20	0.10 ± 0.28	4920 ± 36	2.88 ± 0.07	1.47 ± 0.04	0.06 ± 0.03	4840 ± 47	2.72 ± 0.10	1.47 ± 0.05	0.00 ± 0.04
83465	4712 ± 84	2.58 ± 0.17	1.49 ± 0.10	−0.10 ± 0.07	4839 ± 31	2.67 ± 0.06	1.56 ± 0.03	−0.08 ± 0.03	4837 ± 43	2.72 ± 0.10	1.52 ± 0.04	−0.06 ± 0.03
84698	4846 ± 59	2.71 ± 0.12	1.37 ± 0.08	0.01 ± 0.05	4947 ± 32	2.81 ± 0.06	1.50 ± 0.03	0.01 ± 0.03	4870 ± 36	2.70 ± 0.08	1.46 ± 0.04	−0.03 ± 0.03
85154	4948 ± 204	2.97 ± 0.41	1.18 ± 0.20	0.09 ± 0.57	5085 ± 31	3.13 ± 0.06	1.32 ± 0.03	0.09 ± 0.03	5041 ± 39	3.06 ± 0.08	1.34 ± 0.04	0.07 ± 0.03
85250	5034 ± 60	3.17 ± 0.10	1.35 ± 0.09	0.10 ± 0.06	5119 ± 27	3.16 ± 0.05	1.35 ± 0.03	0.09 ± 0.02	5084 ± 28	3.07 ± 0.07	1.33 ± 0.03	0.08 ± 0.02
85396	5018 ± 64	3.20 ± 0.10	1.20 ± 0.10	−0.15 ± 0.06	5084 ± 18	3.22 ± 0.03	1.20 ± 0.02	−0.15 ± 0.01	5082 ± 19	3.20 ± 0.06	1.21 ± 0.02	−0.15 ± 0.02
85612	5028 ± 80	3.35 ± 0.14	1.14 ± 0.12	−0.04 ± 0.07	5108 ± 22	3.38 ± 0.04	1.18 ± 0.03	−0.05 ± 0.02	5068 ± 22	3.26 ± 0.09	1.20 ± 0.03	−0.08 ± 0.02
87540	4936 ± 223	2.93 ± 0.52	1.18 ± 0.20	0.11 ± 0.18	4959 ± 26	2.85 ± 0.06	1.45 ± 0.03	−0.02 ± 0.02	4914 ± 30	2.71 ± 0.09	1.43 ± 0.03	−0.05 ± 0.03
87627	4713 ± 48	2.60 ± 0.09	1.57 ± 0.06	−0.16 ± 0.04	4778 ± 31	2.56 ± 0.06	1.55 ± 0.03	−0.16 ± 0.03	4741 ± 39	2.50 ± 0.09	1.48 ± 0.04	−0.17 ± 0.03
87816	4904 ± 202	2.79 ± 0.42	1.20 ± 0.20	0.18 ± 0.46	4996 ± 50	2.88 ± 0.09	1.40 ± 0.05	0.13 ± 0.03	4987 ± 55	2.89 ± 0.11	1.37 ± 0.07	0.14 ± 0.04
87896[a]	5260 ± 73	3.65 ± 0.15	1.52 ± 0.14	0.09 ± 0.07	5324 ± 37	3.46 ± 0.09	1.51 ± 0.04	0.13 ± 0.03	5283 ± 46	3.41 ± 0.10	1.45 ± 0.05	0.10 ± 0.04
88323	4953 ± 70	2.76 ± 0.11	1.45 ± 0.09	0.08 ± 0.07	5074 ± 35	2.80 ± 0.07	1.59 ± 0.04	0.09 ± 0.03	5048 ± 43	2.72 ± 0.12	1.52 ± 0.04	0.10 ± 0.04
88836	5047 ± 233	2.88 ± 0.47	1.13 ± 0.20	0.06 ± 0.40	5058 ± 22	2.95 ± 0.05	1.42 ± 0.02	−0.04 ± 0.02	5037 ± 26	2.87 ± 0.08	1.40 ± 0.03	−0.05 ± 0.02
89015	4783 ± 209	2.71 ± 0.42	1.26 ± 0.20	0.09 ± 0.06	4837 ± 36	2.71 ± 0.07	1.56 ± 0.04	−0.02 ± 0.03	4796 ± 38	2.64 ± 0.09	1.48 ± 0.04	−0.01 ± 0.03
90074	5128 ± 59	3.17 ± 0.09	1.22 ± 0.10	0.00 ± 0.06	5197 ± 19	3.17 ± 0.05	1.30 ± 0.02	−0.03 ± 0.02	5164 ± 23	3.06 ± 0.07	1.29 ± 0.03	−0.05 ± 0.02
90317	4890 ± 202	3.41 ± 0.40	1.21 ± 0.20	0.04 ± 0.31	4888 ± 24	3.15 ± 0.06	1.14 ± 0.03	−0.02 ± 0.02	4868 ± 30	3.16 ± 0.07	1.08 ± 0.03	0.00 ± 0.02
90980	4788 ± 201	2.71 ± 0.40	1.26 ± 0.20	0.17 ± 0.74	4967 ± 35	2.98 ± 0.07	1.45 ± 0.04	0.15 ± 0.03	4915 ± 46	2.99 ± 0.11	1.49 ± 0.05	0.11 ± 0.04
91437	5092 ± 63	3.03 ± 0.09	1.33 ± 0.09	0.04 ± 0.06	5178 ± 29	3.09 ± 0.04	1.40 ± 0.03	0.04 ± 0.03	5142 ± 27	2.99 ± 0.08	1.38 ± 0.03	0.02 ± 0.03
93410	4691 ± 69	2.82 ± 0.14	1.30 ± 0.08	−0.20 ± 0.05	4774 ± 33	2.80 ± 0.06	1.32 ± 0.03	−0.20 ± 0.02	4730 ± 35	2.80 ± 0.10	1.30 ± 0.03	−0.22 ± 0.02
93773	5018 ± 54	3.03 ± 0.10	1.47 ± 0.09	−0.02 ± 0.05	5055 ± 27	2.93 ± 0.06	1.42 ± 0.03	−0.05 ± 0.02	5018 ± 29	2.79 ± 0.08	1.42 ± 0.03	−0.07 ± 0.02
94510	4948 ± 65	3.15 ± 0.11	1.28 ± 0.09	−0.12 ± 0.06	5015 ± 24	3.14 ± 0.05	1.24 ± 0.03	−0.12 ± 0.02	5002 ± 24	3.08 ± 0.07	1.24 ± 0.03	−0.13 ± 0.02
94890	4787 ± 202	2.60 ± 0.41	1.26 ± 0.20	0.06 ± 0.31	4911 ± 34	2.76 ± 0.06	1.53 ± 0.03	−0.03 ± 0.03	4892 ± 42	2.76 ± 0.09	1.52 ± 0.04	−0.03 ± 0.03
96566	4910 ± 120	2.56 ± 0.18	1.67 ± 0.18	0.05 ± 0.12	4914 ± 48	2.45 ± 0.10	1.80 ± 0.05	0.00 ± 0.04	4968 ± 49	2.59 ± 0.17	1.75 ± 0.05	0.05 ± 0.05
97344	5009 ± 63	2.96 ± 0.10	1.48 ± 0.11	−0.05 ± 0.06	5130 ± 28	3.09 ± 0.06	1.44 ± 0.03	0.00 ± 0.03	5074 ± 32	3.04 ± 0.12	1.40 ± 0.04	−0.03 ± 0.03
98732	4732 ± 203	3.08 ± 0.41	1.29 ± 0.20	−0.31 ± 0.29	4815 ± 28	3.07 ± 0.05	1.14 ± 0.03	−0.29 ± 0.02	4790 ± 25	3.06 ± 0.05	1.09 ± 0.03	−0.29 ± 0.02
100708	4717 ± 82	2.94 ± 0.15	1.15 ± 0.09	−0.01 ± 0.06	4828 ± 38	3.01 ± 0.07	1.33 ± 0.04	−0.07 ± 0.03	4798 ± 36	2.82 ± 0.16	1.26 ± 0.04	−0.08 ± 0.03
101162	4889 ± 65	2.91 ± 0.11	1.46 ± 0.08	0.08 ± 0.05	4925 ± 32	2.81 ± 0.06	1.47 ± 0.04	0.05 ± 0.03	4936 ± 31	2.79 ± 0.17	1.48 ± 0.04	0.06 ± 0.03
103462	4950 ± 92	2.53 ± 0.11	1.41 ± 0.43	−0.53 ± 0.10	5068 ± 15	2.75 ± 0.04	1.56 ± 0.02	−0.47 ± 0.01	5100 ± 21	2.79 ± 0.06	1.57 ± 0.03	−0.45 ± 0.02
104704	4716 ± 86	3.04 ± 0.17	1.23 ± 0.10	−0.09 ± 0.06	4775 ± 30	2.93 ± 0.06	1.24 ± 0.03	−0.15 ± 0.02	4736 ± 40	2.85 ± 0.09	1.20 ± 0.04	−0.16 ± 0.03
106572	4722 ± 110	2.38 ± 0.18	1.50 ± 0.32	−0.49 ± 0.09	4825 ± 26	2.53 ± 0.05	1.61 ± 0.03	−0.44 ± 0.02	4806 ± 27	2.52 ± 0.07	1.62 ± 0.03	−0.46 ± 0.02
110829	4883 ± 202	3.41 ± 0.40	1.21 ± 0.20	0.23 ± 0.63	4844 ± 43	3.01 ± 0.09	1.30 ± 0.04	0.10 ± 0.03	4824 ± 44	2.79 ± 0.22	1.30 ± 0.05	0.07 ± 0.03
111295	4853 ± 101	2.40 ± 0.15	1.47 ± 0.34	−0.41 ± 0.09	5049 ± 27	2.88 ± 0.06	1.78 ± 0.03	−0.32 ± 0.03	5029 ± 34	2.79 ± 0.12	1.69 ± 0.05	−0.33 ± 0.03
113778	4736 ± 118	2.62 ± 0.22	1.49 ± 0.16	−0.07 ± 0.10	4842 ± 32	2.72 ± 0.07	1.52 ± 0.03	−0.05 ± 0.03	4821 ± 38	2.60 ± 0.10	1.49 ± 0.04	−0.07 ± 0.03
114474	4831 ± 82	3.02 ± 0.15	1.34 ± 0.10	0.14 ± 0.06	4842 ± 41	2.83 ± 0.07	1.47 ± 0.04	0.03 ± 0.03	4790 ± 48	2.76 ± 0.10	1.41 ± 0.05	0.03 ± 0.03
115310	5079 ± 94	3.15 ± 0.13	1.41 ± 0.16	0.10 ± 0.10	5097 ± 28	2.97 ± 0.05	1.43 ± 0.03	0.04 ± 0.03	5011 ± 34	2.80 ± 0.07	1.45 ± 0.04	−0.03 ± 0.03
116243[a]	5058 ± 101	2.69 ± 0.12	1.91 ± 0.33	−0.34 ± 0.12	5325 ± 22	3.02 ± 0.05	1.63 ± 0.03	−0.12 ± 0.02	5305 ± 32	2.97 ± 0.10	1.62 ± 0.04	−0.13 ± 0.03
118338	5031 ± 397	2.90 ± 0.80	1.13 ± 0.20	0.17 ± 0.89	5178 ± 25	3.13 ± 0.05	1.47 ± 0.03	0.10 ± 0.02	5131 ± 32	3.10 ± 0.13	1.44 ± 0.04	0.08 ± 0.03
119250	4821 ± 97	2.68 ± 0.16	1.44 ± 0.13	−0.14 ± 0.09	4882 ± 27	2.67 ± 0.05	1.50 ± 0.03	−0.15 ± 0.02	4823 ± 37	2.50 ± 0.10	1.47 ± 0.04	−0.18 ± 0.03
120457	4916 ± 203	2.95 ± 0.41	1.19 ± 0.20	0.23 ± 0.74	5042 ± 32	3.09 ± 0.07	1.39 ± 0.03	0.16 ± 0.02	5017 ± 42	3.08 ± 0.08	1.33 ± 0.05	0.17 ± 0.03
121853	4934 ± 67	2.76 ± 0.10	1.50 ± 0.14	−0.28 ± 0.07	4985 ± 23	2.77 ± 0.04	1.57 ± 0.03	−0.28 ± 0.02	4968 ± 24	2.68 ± 0.06	1.50 ± 0.03	−0.28 ± 0.02
123151	4864 ± 66	2.72 ± 0.10	1.42 ± 0.09	−0.18 ± 0.06	4971 ± 29	2.80 ± 0.05	1.51 ± 0.04	−0.19 ± 0.02	4957 ± 35	2.77 ± 0.10	1.48 ± 0.04	−0.19 ± 0.03
123569	4981 ± 202	2.94 ± 0.40	1.16 ± 0.20	0.11 ± 0.71	5104 ± 27	3.12 ± 0.05	1.37 ± 0.03	0.07 ± 0.02	5089 ± 31	3.13 ± 0.08	1.38 ± 0.03	0.07 ± 0.03
125136	4781 ± 163	2.96 ± 0.30	1.42 ± 0.21	−0.16 ± 0.14	4949 ± 33	3.15 ± 0.06	1.18 ± 0.04	−0.01 ± 0.02	4937 ± 37	2.97 ± 0.20	1.22 ± 0.04	−0.05 ± 0.03
127195	4947 ± 66	3.42 ± 0.11	1.10 ± 0.10	−0.05 ± 0.05	5006 ± 23	3.37 ± 0.04	1.09 ± 0.03	−0.07 ± 0.02	4990 ± 24	3.38 ± 0.05	1.09 ± 0.03	−0.08 ± 0.02

Table 1. – *continued*

HD number	HM07 line-list $T_{\rm eff}$ (K)	HM07 line-list log g (cm s^{-2})	HM07 line-list ξ (km s^{-1})	HM07 line-list [Fe/H] (dex)	S08 line-list $T_{\rm eff}$ (K)	S08 line-list log g (cm s^{-2})	S08 line-list ξ (km s^{-1})	S08 line-list [Fe/H] (dex)	T13 line-list $T_{\rm eff}$ (K)	T13 line-list log g (cm s^{-2})	T13 line-list ξ (km s^{-1})	T13 line-list [Fe/H] (dex)
129462	4915 ± 165	3.00 ± 0.25	2.04 ± 0.31	−0.16 ± 0.14	4985 ± 27	2.84 ± 0.04	1.52 ± 0.03	−0.07 ± 0.02	4953 ± 26	2.75 ± 0.06	1.48 ± 0.03	−0.08 ± 0.02
129893	4914 ± 59	2.91 ± 0.10	1.43 ± 0.08	0.01 ± 0.05	4974 ± 31	2.88 ± 0.05	1.44 ± 0.03	−0.01 ± 0.03	4917 ± 35	2.80 ± 0.08	1.40 ± 0.04	−0.03 ± 0.03
130650	4940 ± 71	2.79 ± 0.11	1.51 ± 0.12	−0.07 ± 0.07	5027 ± 24	2.78 ± 0.04	1.54 ± 0.03	−0.06 ± 0.02	5009 ± 28	2.79 ± 0.07	1.51 ± 0.03	−0.06 ± 0.02
131376	5052 ± 234	3.01 ± 0.47	1.12 ± 0.20	0.14 ± 0.59	5126 ± 26	3.11 ± 0.06	1.43 ± 0.03	0.08 ± 0.02	5096 ± 34	3.06 ± 0.08	1.42 ± 0.03	0.07 ± 0.03
132905	4876 ± 66	2.54 ± 0.09	1.46 ± 0.12	−0.39 ± 0.07	4954 ± 22	2.69 ± 0.05	1.53 ± 0.02	−0.37 ± 0.02	4989 ± 22	2.61 ± 0.18	1.55 ± 0.03	−0.35 ± 0.02
133921[a]	5173 ± 60	3.10 ± 0.11	1.15 ± 0.09	0.15 ± 0.06	5283 ± 31	3.10 ± 0.09	1.24 ± 0.03	0.18 ± 0.03	5270 ± 38	3.10 ± 0.12	1.18 ± 0.04	0.18 ± 0.04
134505	5101 ± 247	2.92 ± 0.50	1.10 ± 0.20	0.09 ± 0.10	5156 ± 24	3.07 ± 0.04	1.44 ± 0.03	0.02 ± 0.02	5126 ± 23	3.01 ± 0.06	1.42 ± 0.03	0.00 ± 0.02
135760	4801 ± 201	3.41 ± 0.40	1.25 ± 0.20	0.21 ± 0.59	4891 ± 71	3.32 ± 0.14	1.24 ± 0.07	0.19 ± 0.04	4909 ± 94	3.49 ± 0.19	1.06 ± 0.09	0.27 ± 0.05
136014	4807 ± 73	2.57 ± 0.12	1.56 ± 0.13	−0.49 ± 0.07	4925 ± 21	2.73 ± 0.04	1.62 ± 0.02	−0.43 ± 0.02	4899 ± 23	2.69 ± 0.07	1.63 ± 0.03	−0.46 ± 0.02
136672	4763 ± 266	2.59 ± 0.53	1.27 ± 0.20	−0.29 ± 0.20	4842 ± 31	2.68 ± 0.06	1.53 ± 0.03	−0.33 ± 0.03	4829 ± 27	2.68 ± 0.09	1.48 ± 0.03	−0.32 ± 0.02
139521	4888 ± 52	2.76 ± 0.09	1.52 ± 0.08	−0.14 ± 0.05	4954 ± 24	2.75 ± 0.04	1.50 ± 0.03	−0.13 ± 0.02	4960 ± 27	2.79 ± 0.07	1.45 ± 0.03	−0.11 ± 0.02
139980	4885 ± 212	2.67 ± 0.44	1.21 ± 0.20	−0.07 ± 0.21	4944 ± 28	2.87 ± 0.06	1.47 ± 0.03	−0.15 ± 0.02	4936 ± 25	2.83 ± 0.08	1.45 ± 0.03	−0.14 ± 0.02
140329	4991 ± 201	3.45 ± 0.40	1.15 ± 0.20	0.07 ± 0.85	5043 ± 30	3.40 ± 0.07	1.15 ± 0.04	0.02 ± 0.02	4988 ± 32	3.31 ± 0.10	1.09 ± 0.04	0.01 ± 0.02
140861	5032 ± 87	2.76 ± 0.13	2.02 ± 0.26	−0.39 ± 0.10	5069 ± 18	2.69 ± 0.04	1.75 ± 0.02	−0.36 ± 0.02	5082 ± 20	2.71 ± 0.08	1.76 ± 0.03	−0.36 ± 0.02
141832	4972 ± 202	3.45 ± 0.40	1.16 ± 0.20	0.19 ± 0.94	5046 ± 43	3.41 ± 0.07	1.30 ± 0.05	0.11 ± 0.04	4936 ± 50	3.43 ± 0.25	1.11 ± 0.06	0.13 ± 0.03
143009	5029 ± 224	2.63 ± 0.45	1.14 ± 0.20	0.18 ± 0.60	5067 ± 27	2.77 ± 0.05	1.68 ± 0.03	0.04 ± 0.03	4994 ± 36	2.69 ± 0.12	1.63 ± 0.04	0.00 ± 0.03
143546[a]	5152 ± 222	3.05 ± 0.45	1.07 ± 0.20	0.15 ± 0.75	5223 ± 28	3.11 ± 0.06	1.52 ± 0.03	0.05 ± 0.03	5212 ± 39	3.07 ± 0.12	1.44 ± 0.04	0.06 ± 0.04
145621	4754 ± 53	2.76 ± 0.12	1.54 ± 0.07	−0.02 ± 0.04	4854 ± 44	2.75 ± 0.08	1.56 ± 0.04	−0.01 ± 0.03	4739 ± 42	2.85 ± 0.27	1.48 ± 0.04	−0.01 ± 0.03
146686	4755 ± 204	2.88 ± 0.41	1.28 ± 0.20	0.37 ± 0.71	4914 ± 71	2.95 ± 0.12	1.44 ± 0.07	0.27 ± 0.04	4813 ± 75	2.73 ± 0.16	1.37 ± 0.08	0.25 ± 0.05
146690	4938 ± 201	2.75 ± 0.40	1.18 ± 0.20	0.11 ± 0.82	5050 ± 28	2.91 ± 0.05	1.46 ± 0.03	0.04 ± 0.02	5023 ± 31	2.84 ± 0.07	1.46 ± 0.03	0.02 ± 0.03
148890	5037 ± 204	2.87 ± 0.41	1.13 ± 0.20	0.08 ± 0.74	5069 ± 26	2.91 ± 0.05	1.45 ± 0.03	−0.01 ± 0.02	5039 ± 31	2.81 ± 0.08	1.47 ± 0.03	−0.05 ± 0.03
155276	4717 ± 237	2.63 ± 0.47	1.29 ± 0.20	0.18 ± 0.43	4943 ± 53	2.96 ± 0.10	1.51 ± 0.05	0.17 ± 0.04	4851 ± 60	2.86 ± 0.13	1.43 ± 0.06	0.17 ± 0.04
156854	4863 ± 343	2.79 ± 0.69	1.22 ± 0.20	0.10 ± 1.43	4981 ± 32	2.90 ± 0.06	1.53 ± 0.04	0.00 ± 0.03	4883 ± 42	2.70 ± 0.12	1.44 ± 0.04	−0.05 ± 0.03
157515	4885 ± 57	3.27 ± 0.10	1.17 ± 0.08	−0.11 ± 0.05	4911 ± 26	3.19 ± 0.06	1.16 ± 0.03	−0.16 ± 0.02	4892 ± 25	3.17 ± 0.07	1.12 ± 0.03	−0.16 ± 0.02
159558	4825 ± 66	2.65 ± 0.11	1.59 ± 0.11	−0.30 ± 0.06	4889 ± 22	2.64 ± 0.04	1.55 ± 0.03	−0.29 ± 0.02	4861 ± 25	2.46 ± 0.13	1.52 ± 0.03	−0.31 ± 0.02
160720	5125 ± 92	3.11 ± 0.13	1.50 ± 0.15	0.03 ± 0.09	5235 ± 30	3.08 ± 0.06	1.51 ± 0.03	0.04 ± 0.03	5177 ± 29	2.94 ± 0.10	1.46 ± 0.03	0.00 ± 0.03
160819	4877 ± 205	3.24 ± 0.41	1.21 ± 0.20	0.03 ± 0.09	4893 ± 30	3.08 ± 0.06	1.28 ± 0.03	−0.08 ± 0.02	4822 ± 47	3.23 ± 0.29	1.12 ± 0.05	−0.03 ± 0.03
161814	4853 ± 204	2.70 ± 0.41	1.23 ± 0.20	0.15 ± 0.23	4955 ± 36	2.80 ± 0.06	1.47 ± 0.03	0.10 ± 0.03	4911 ± 42	2.71 ± 0.10	1.46 ± 0.04	0.08 ± 0.03
163652	4944 ± 75	2.68 ± 0.11	1.61 ± 0.18	−0.40 ± 0.09	5011 ± 16	2.73 ± 0.03	1.53 ± 0.02	−0.36 ± 0.01	5014 ± 19	2.73 ± 0.04	1.54 ± 0.02	−0.36 ± 0.02
165135	4774 ± 59	2.68 ± 0.11	1.39 ± 0.08	−0.24 ± 0.05	4875 ± 29	2.79 ± 0.05	1.40 ± 0.03	−0.19 ± 0.02	4860 ± 32	2.74 ± 0.07	1.38 ± 0.03	−0.20 ± 0.03
165634	4950 ± 62	2.58 ± 0.09	1.55 ± 0.10	−0.03 ± 0.07	5061 ± 25	2.73 ± 0.06	1.62 ± 0.03	−0.01 ± 0.02	5062 ± 26	2.58 ± 0.10	1.63 ± 0.03	−0.01 ± 0.03
166063	5009 ± 207	2.32 ± 0.42	1.15 ± 0.20	0.13 ± 0.46	5035 ± 34	2.37 ± 0.08	1.98 ± 0.04	−0.07 ± 0.03	4996 ± 42	2.32 ± 0.12	1.85 ± 0.05	−0.07 ± 0.04
166599	5088 ± 221	3.14 ± 0.44	1.10 ± 0.20	0.15 ± 0.66	5076 ± 28	3.01 ± 0.05	1.39 ± 0.03	0.01 ± 0.02	5052 ± 27	2.94 ± 0.08	1.39 ± 0.03	0.00 ± 0.02
166949	5123 ± 210	3.35 ± 0.42	1.09 ± 0.20	0.00 ± 0.64	5166 ± 21	3.27 ± 0.05	1.27 ± 0.02	−0.05 ± 0.02	5130 ± 22	3.26 ± 0.12	1.22 ± 0.03	−0.06 ± 0.02
168838	4817 ± 206	2.66 ± 0.41	1.24 ± 0.20	0.12 ± 0.49	5028 ± 36	2.99 ± 0.07	1.52 ± 0.04	0.12 ± 0.03	4930 ± 42	2.79 ± 0.10	1.43 ± 0.04	0.09 ± 0.03
169767	4782 ± 65	2.94 ± 0.13	1.30 ± 0.08	−0.13 ± 0.05	4821 ± 30	2.84 ± 0.06	1.33 ± 0.03	−0.19 ± 0.02	4801 ± 39	2.78 ± 0.09	1.28 ± 0.04	−0.19 ± 0.03
169836	4870 ± 205	2.70 ± 0.48	1.22 ± 0.20	0.05 ± 0.29	4993 ± 27	2.86 ± 0.05	1.48 ± 0.03	−0.01 ± 0.02	4934 ± 34	2.75 ± 0.08	1.48 ± 0.04	−0.05 ± 0.03
169916	4793 ± 205	3.03 ± 0.41	1.26 ± 0.20	0.04 ± 0.49	4801 ± 32	2.81 ± 0.07	1.35 ± 0.03	−0.08 ± 0.03	4778 ± 37	2.59 ± 0.18	1.35 ± 0.04	−0.11 ± 0.03
172211	4996 ± 202	2.85 ± 0.41	1.15 ± 0.20	0.32 ± 1.08	5115 ± 34	2.99 ± 0.06	1.53 ± 0.03	0.17 ± 0.03	5082 ± 34	2.94 ± 0.09	1.47 ± 0.04	0.18 ± 0.03
172875	4975 ± 78	3.04 ± 0.12	1.43 ± 0.12	0.08 ± 0.07	5070 ± 33	3.04 ± 0.06	1.46 ± 0.04	0.11 ± 0.03	5026 ± 45	2.99 ± 0.09	1.38 ± 0.05	0.11 ± 0.04
173378	4926 ± 62	3.19 ± 0.10	1.23 ± 0.09	−0.21 ± 0.05	5005 ± 19	3.17 ± 0.04	1.18 ± 0.02	−0.20 ± 0.02	4994 ± 20	3.17 ± 0.04	1.17 ± 0.02	−0.20 ± 0.02
173540[a]	5511 ± 123	3.76 ± 0.15	2.89 ± 1.46	−0.24 ± 0.18	5547 ± 31	3.32 ± 0.07	1.74 ± 0.04	−0.15 ± 0.03	5591 ± 46	3.48 ± 0.12	1.86 ± 0.08	−0.15 ± 0.04
174295	4854 ± 72	2.67 ± 0.12	1.39 ± 0.09	−0.19 ± 0.07	4974 ± 24	2.84 ± 0.06	1.44 ± 0.03	−0.17 ± 0.02	4960 ± 28	2.61 ± 0.14	1.46 ± 0.03	−0.20 ± 0.03
175145[a]	5374 ± 163	3.69 ± 0.23	1.20 ± 0.32	0.16 ± 0.17	5382 ± 23	3.49 ± 0.06	1.41 ± 0.03	0.02 ± 0.02	5348 ± 28	3.44 ± 0.12	1.33 ± 0.04	0.01 ± 0.03

Table 1. – *continued*

HD number	HM07 line-list $T_{\rm eff}$ (K)	HM07 line-list log g (cm s^{-2})	HM07 line-list ξ (km s^{-1})	HM07 line-list [Fe/H] (dex)	S08 line-list $T_{\rm eff}$ (K)	S08 line-list log g (cm s^{-2})	S08 line-list ξ (km s^{-1})	S08 line-list [Fe/H] (dex)	T13 line-list $T_{\rm eff}$ (K)	T13 line-list log g (cm s^{-2})	T13 line-list ξ (km s^{-1})	T13 line-list [Fe/H] (dex)
175219	4800 ± 63	2.56 ± 0.10	1.49 ± 0.09	−0.31 ± 0.06	4896 ± 25	2.71 ± 0.05	1.50 ± 0.03	−0.29 ± 0.02	4888 ± 30	2.64 ± 0.06	1.52 ± 0.04	−0.30 ± 0.03
175401	5009 ± 86	2.98 ± 0.14	1.79 ± 0.15	0.04 ± 0.08	5102 ± 37	2.97 ± 0.06	1.57 ± 0.04	0.16 ± 0.03	5042 ± 42	2.79 ± 0.12	1.55 ± 0.04	0.12 ± 0.04
177222	4914 ± 59	3.00 ± 0.09	1.28 ± 0.08	−0.03 ± 0.06	4993 ± 26	3.00 ± 0.06	1.38 ± 0.03	−0.06 ± 0.02	4952 ± 32	2.84 ± 0.13	1.34 ± 0.03	−0.08 ± 0.03
177389	5049 ± 67	3.52 ± 0.10	1.09 ± 0.10	−0.01 ± 0.05	5102 ± 24	3.50 ± 0.04	1.08 ± 0.03	−0.03 ± 0.02	5061 ± 26	3.49 ± 0.09	1.05 ± 0.03	−0.05 ± 0.02
179433	5291 ± 220	3.49 ± 0.44	1.00 ± 0.20	0.28 ± 0.57	5168 ± 22	3.15 ± 0.04	1.38 ± 0.02	−0.02 ± 0.02	5145 ± 31	3.16 ± 0.08	1.39 ± 0.04	−0.04 ± 0.03
181517	4965 ± 209	2.95 ± 0.42	1.17 ± 0.20	0.18 ± 0.29	5050 ± 33	2.99 ± 0.06	1.47 ± 0.03	0.08 ± 0.03	4996 ± 41	2.96 ± 0.08	1.44 ± 0.05	0.07 ± 0.03
182893	4913 ± 201	3.04 ± 0.49	1.19 ± 0.20	0.19 ± 0.37	5043 ± 30	3.13 ± 0.06	1.38 ± 0.03	0.14 ± 0.02	4994 ± 40	3.09 ± 0.09	1.36 ± 0.04	0.12 ± 0.03
185075	4703 ± 64	2.58 ± 0.11	1.39 ± 0.10	−0.49 ± 0.06	4792 ± 27	2.67 ± 0.05	1.41 ± 0.03	−0.47 ± 0.02	4749 ± 23	2.55 ± 0.05	1.39 ± 0.03	−0.51 ± 0.02
189005[a]	5086 ± 72	2.67 ± 0.09	1.63 ± 0.15	−0.21 ± 0.08	5222 ± 20	2.90 ± 0.04	1.69 ± 0.02	−0.15 ± 0.02	5203 ± 25	2.88 ± 0.07	1.67 ± 0.03	−0.16 ± 0.03
189080	4716 ± 201	2.81 ± 0.40	1.29 ± 0.20	−0.09 ± 0.31	4791 ± 34	2.81 ± 0.06	1.40 ± 0.03	−0.13 ± 0.02	4720 ± 34	2.71 ± 0.10	1.34 ± 0.03	−0.15 ± 0.02
189195	4864 ± 60	2.75 ± 0.10	1.44 ± 0.09	−0.10 ± 0.06	4936 ± 24	2.78 ± 0.05	1.47 ± 0.03	−0.11 ± 0.02	4887 ± 29	2.68 ± 0.07	1.47 ± 0.03	−0.14 ± 0.03
195569	4852 ± 77	2.84 ± 0.15	1.39 ± 0.10	0.00 ± 0.06	4948 ± 31	2.84 ± 0.06	1.46 ± 0.03	−0.02 ± 0.03	4909 ± 33	2.83 ± 0.08	1.44 ± 0.03	−0.02 ± 0.03
196171	4859 ± 57	2.79 ± 0.10	1.43 ± 0.08	−0.06 ± 0.05	4941 ± 33	2.83 ± 0.05	1.44 ± 0.03	−0.05 ± 0.03	4900 ± 43	2.83 ± 0.10	1.43 ± 0.04	−0.07 ± 0.03
198232	4877 ± 63	2.39 ± 0.25	1.43 ± 0.09	−0.01 ± 0.07	4948 ± 35	2.65 ± 0.07	1.59 ± 0.04	−0.02 ± 0.03	4898 ± 43	2.37 ± 0.18	1.51 ± 0.04	−0.05 ± 0.04
199951[a]	5088 ± 91	2.81 ± 0.15	1.37 ± 0.18	−0.09 ± 0.10	5279 ± 30	3.06 ± 0.09	1.62 ± 0.04	−0.01 ± 0.03	5242 ± 32	3.02 ± 0.15	1.52 ± 0.04	−0.02 ± 0.03
201852	5025 ± 243	3.02 ± 0.48	1.14 ± 0.20	0.11 ± 0.13	5038 ± 24	3.01 ± 0.05	1.42 ± 0.03	0.00 ± 0.02	4999 ± 34	3.05 ± 0.10	1.41 ± 0.04	−0.02 ± 0.03
207229	4896 ± 210	2.83 ± 0.42	1.20 ± 0.20	0.11 ± 0.15	4947 ± 34	2.83 ± 0.06	1.52 ± 0.04	0.00 ± 0.03	4887 ± 39	2.71 ± 0.09	1.46 ± 0.04	−0.02 ± 0.03
207883	4822 ± 61	2.61 ± 0.10	1.47 ± 0.09	−0.22 ± 0.06	4934 ± 25	2.74 ± 0.05	1.53 ± 0.03	−0.20 ± 0.02	4911 ± 28	2.75 ± 0.06	1.49 ± 0.03	−0.20 ± 0.02
208285	4850 ± 72	2.67 ± 0.12	1.67 ± 0.15	−0.50 ± 0.07	4953 ± 21	2.80 ± 0.04	1.62 ± 0.02	−0.43 ± 0.02	4947 ± 25	2.77 ± 0.05	1.60 ± 0.03	−0.44 ± 0.02
208737	4888 ± 75	2.56 ± 0.13	1.60 ± 0.10	−0.02 ± 0.07	5025 ± 32	2.71 ± 0.06	1.62 ± 0.03	0.05 ± 0.03	4968 ± 34	2.68 ± 0.10	1.59 ± 0.04	0.03 ± 0.03
210056	4819 ± 234	3.02 ± 0.47	1.24 ± 0.20	−0.06 ± 0.28	4870 ± 34	3.00 ± 0.07	1.31 ± 0.03	−0.10 ± 0.02	4824 ± 29	2.99 ± 0.10	1.25 ± 0.03	−0.10 ± 0.02
210622	4953 ± 201	3.35 ± 0.40	1.17 ± 0.20	0.06 ± 0.85	5033 ± 26	3.34 ± 0.06	1.18 ± 0.03	0.05 ± 0.02	4999 ± 31	3.19 ± 0.14	1.18 ± 0.04	0.03 ± 0.02
212953	4812 ± 77	2.62 ± 0.11	1.52 ± 0.13	−0.43 ± 0.07	4896 ± 23	2.68 ± 0.05	1.56 ± 0.03	−0.41 ± 0.02	4893 ± 24	2.63 ± 0.08	1.55 ± 0.03	−0.41 ± 0.02
213009	4816 ± 146	2.47 ± 0.26	2.08 ± 0.25	−0.22 ± 0.14	5045 ± 59	2.93 ± 0.12	2.23 ± 0.08	−0.12 ± 0.06	5013 ± 88	2.54 ± 0.28	2.39 ± 0.14	−0.23 ± 0.09
214462	4762 ± 53	2.86 ± 0.11	1.28 ± 0.06	−0.03 ± 0.04	4831 ± 36	2.88 ± 0.08	1.35 ± 0.03	−0.07 ± 0.03	4770 ± 44	2.76 ± 0.10	1.30 ± 0.04	−0.09 ± 0.03
215104	4755 ± 83	2.55 ± 0.15	1.61 ± 0.12	−0.20 ± 0.08	4918 ± 30	2.77 ± 0.06	1.51 ± 0.03	−0.11 ± 0.02	4882 ± 34	2.70 ± 0.07	1.49 ± 0.04	−0.13 ± 0.03
215682	4715 ± 55	2.64 ± 0.10	1.50 ± 0.07	−0.09 ± 0.05	4795 ± 38	2.66 ± 0.07	1.51 ± 0.04	−0.10 ± 0.03	4728 ± 43	2.51 ± 0.10	1.50 ± 0.04	−0.15 ± 0.03
216210	5095 ± 60	3.19 ± 0.09	1.28 ± 0.10	−0.01 ± 0.06	5166 ± 20	3.22 ± 0.03	1.28 ± 0.02	0.00 ± 0.02	5135 ± 26	3.14 ± 0.07	1.30 ± 0.03	−0.03 ± 0.02
216742	4825 ± 66	3.05 ± 0.11	1.30 ± 0.09	−0.11 ± 0.05	4836 ± 32	2.90 ± 0.06	1.34 ± 0.03	−0.18 ± 0.02	4812 ± 34	2.86 ± 0.07	1.31 ± 0.04	−0.18 ± 0.02
216763	4902 ± 65	2.80 ± 0.11	1.50 ± 0.09	−0.18 ± 0.06	4984 ± 23	2.86 ± 0.05	1.46 ± 0.03	−0.14 ± 0.02	4980 ± 32	2.87 ± 0.08	1.47 ± 0.03	−0.14 ± 0.03
219507	4711 ± 56	2.71 ± 0.11	1.47 ± 0.07	−0.09 ± 0.04	4819 ± 35	2.73 ± 0.07	1.50 ± 0.04	−0.10 ± 0.03	4763 ± 44	2.63 ± 0.10	1.50 ± 0.04	−0.14 ± 0.03
219572	5055 ± 58	3.02 ± 0.10	1.49 ± 0.10	−0.04 ± 0.06	5112 ± 23	2.97 ± 0.06	1.44 ± 0.03	−0.03 ± 0.02	5087 ± 28	2.91 ± 0.08	1.44 ± 0.03	−0.04 ± 0.02
220790	4847 ± 204	2.64 ± 0.41	1.23 ± 0.20	−0.17 ± 0.29	4940 ± 25	2.80 ± 0.06	1.51 ± 0.03	−0.19 ± 0.02	4902 ± 27	2.75 ± 0.08	1.48 ± 0.03	−0.21 ± 0.02
221323	4839 ± 205	2.81 ± 0.41	1.23 ± 0.20	0.15 ± 0.06	4919 ± 34	2.82 ± 0.06	1.51 ± 0.04	0.00 ± 0.03	4842 ± 44	2.63 ± 0.09	1.47 ± 0.04	−0.04 ± 0.03
222433	4913 ± 65	2.81 ± 0.10	1.39 ± 0.09	−0.09 ± 0.06	4956 ± 25	2.78 ± 0.06	1.43 ± 0.03	−0.12 ± 0.02	4941 ± 30	2.71 ± 0.07	1.44 ± 0.03	−0.14 ± 0.03
223647	4930 ± 74	2.71 ± 0.11	1.51 ± 0.14	−0.36 ± 0.08	5034 ± 19	2.82 ± 0.04	1.54 ± 0.02	−0.33 ± 0.02	5017 ± 25	2.77 ± 0.07	1.51 ± 0.03	−0.34 ± 0.03
223700	4995 ± 237	3.17 ± 0.47	1.15 ± 0.20	0.17 ± 0.59	5024 ± 30	3.08 ± 0.06	1.33 ± 0.03	0.10 ± 0.02	5018 ± 36	3.09 ± 0.09	1.31 ± 0.04	0.11 ± 0.03
224362	4732 ± 99	2.65 ± 0.20	1.40 ± 0.11	−0.02 ± 0.08	4922 ± 42	2.89 ± 0.08	1.56 ± 0.04	0.02 ± 0.03	4782 ± 42	2.52 ± 0.13	1.51 ± 0.04	−0.07 ± 0.03

Note. [a]For this star the parameters derived with the SO08 line-list may also be adopted as final. See Section 3 for details.

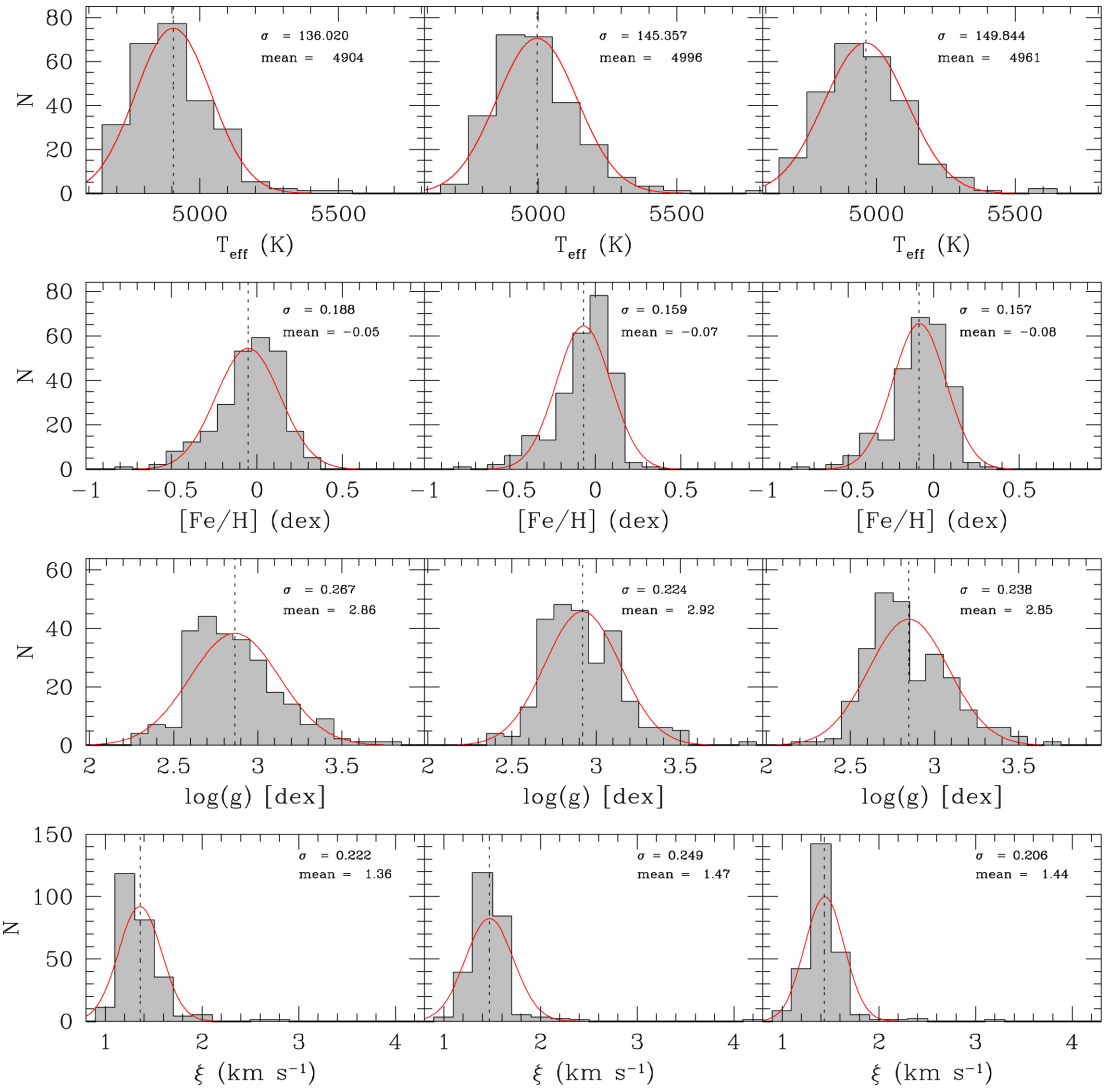

Figure 2. Distribution of the atmospheric parameters derived using the HM07 (left-hand panel), SO08 (middle panel), and TS13 (right-hand panel) line-lists. In each plot, the Gaussian fit to the distribution, along with the values of the mean (dotted line) and the standard deviation σ is also shown.

measurements in the context of the Geneva extrasolar planet search programme. The data were obtained at La Silla Obervatory (Chile), using the Corallie spectrograph (Udry et al. 2000). High-resolution ($\lambda/\Delta\lambda \sim 110\,000$) and high-signal-to-noise (S/N) spectra for all stars in the sample were obtained using the Ultra-violet and Visible Echelle Spectrograph (UVES) (VLT Kueyen Telescope, Paranal, Chile), between 2010 April and December (ESO programmes 085.C-0062 and 086.C-0098). The observations were done using the UVES standard setup Red 580 ($R = 47\,000$, spectral range: 480–680 nm). The final spectra cover the wavelength domain between 4780 and 6805 Å, and have a typical S/N of ∼150. All spectra for each individual star were combined using the IRAF[3] SCOMBINE task. The spectra were reduced using the UVES pipeline.

Fig. 1 presents the distribution of these stars through the H–R diagram. In this figure, the $(B - V)$ colour index was taken from *Hipparcos* (Perryman et al. 1997). The surface luminosity, $\log L/L_{\odot}$, was computed from the estimated *Hipparcos* parallaxes and V magnitude following the calibrations presented by Flower (1996), and revisited by Torres (2010). The evolutionary tracks are from Ekström et al. (2012), for an initial abundance of metals set to $Z = 0.014$. This plot indicate that our sample is composed only by giant stars. As we can see in this figure, the stars in this sample have stellar masses between 1.5 and 4.0 solar masses. For a detailed discussion on mass distribution of (sub-)giant planet hosts, we redirect the reader to Lloyd (2013).

[3] IRAF is distributed by National Optical Astronomy Observatories, operated by the Association of Universities for Research in Astronomy, Inc., under contract with the National Science Foundation, USA.

3 DETERMINATION OF SPECTROSCOPIC PARAMETERS

The atmospheric stellar parameters – the effective temperature $T_{\rm eff}$, the surface gravity $\log g$, the microturbulence ξ, and the metallicity [Fe/H] – were derived following the same procedure described in Santos et al. (2004). Such a procedure is based on the equivalent widths (EW) of Fe I and Fe II lines, and iron excitation and ionization equilibrium, assumed a local thermodynamic equilibrium. For this

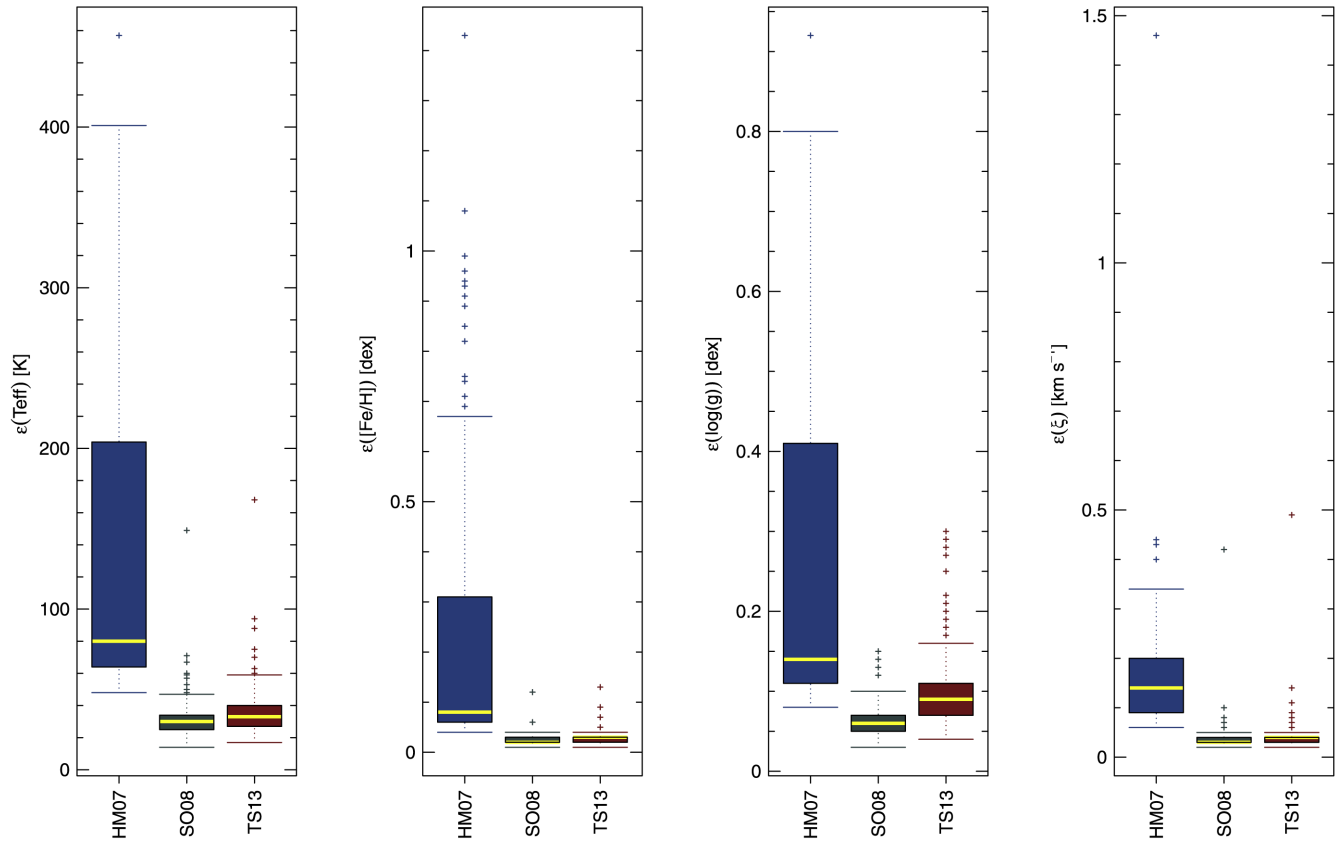

Figure 3. Boxplot showing the median (solid horizontal yellow lines), lower and upper quartiles (box), range of data points within 1.5× (75–25 per cent) range (whiskers), and outliers (individual crosses) of the uncertainties for derived parameters presented in Fig. 2.

mostly automatic analysis, we used the code MOOG[4] (Sneden 1973), with a grid of ATLAS plane-parallel model atmospheres (Kurucz 1993). The EWs were computed by using the code ARES (Automatic Routine for line Equivalent widths in stellar spectra – Sousa et al. 2007).[5] The input parameters for ARES are the same as in Sousa et al. (2008), and the S/N adopted is given as a root sum square of the S/N of the order related to 6000 Å (see UVES ETC)[6], for each spectrum, extracted in the header of the fits reduced spectra. The determination of the uncertainties in the derived parameters also follow the same prescription as in Santos et al. (2004).

The determination of spectroscopic stellar parameters greatly depends on the selection of the Fe lines and the transition probabilities of those lines. For a complete discussion about this dependence and its implications for the study of chemical abundances in giant stars, we direct the reader to Santos et al. (2009). These authors also discuss the implications of a carefully choice of the lines for derivation of metallicities and other stellar parameters. Due to the fact that stellar parameters may depend on the line-list choice, for our analysis we use three different line-lists: the large line-list from Sousa et al. (2008, hereafter SO08), the line-list for cooler stars based on the SO08 line-list (Tsantaki et al. 2013, hereafter TS13), and the small line-list, made specifically for giant stars, from Hekker & Meléndez (2007, hereafter HM07). SO08 is composed by 263 Fe I abd 36 Fe II weak lines, and the transition probabilities (log *gf* values) were determined using a differential analysis to the Sun. The reference solar iron abundance used to make this list is $A(\mathrm{Fe})_{\odot} = 7.47$. TS13 was built from this list, specifically for cooler stars. As only weak and isolated lines were left, to avoid blending effects, the TS13 line-list is composed by 120 Fe I and 17 Fe II lines. The smaller line-list is HM07, with 16 Fe I and 6 Fe II lines. This line-list was specifically made for giant stars and all lines were carefully selected to avoid blends by atomic and CN lines. The log *gf* values are mostly based on different laboratory works (some few cases with small adjustments using the Arcturus atlas), as there is no single source of laboratory log *gf* for either Fe I or Fe II. Unlike the SO08 and TS13 line-lists, the reference value of $A(\mathrm{Fe})_{\odot} = 7.49$ is used. Table 1 lists all stellar parameters derived with the SO08, TS13 and HM07 line-lists. Note that no viable solution could be found for HD 74006 using the HM07 line-list.

As pointed out by TS13 the results from using the SO08 line-list for cool stars ($T_{\rm eff} < 5200$ K) have shown to be unsatisfactory. For those stars, the results found with the TS13 line-list presents a better agreement with the expected value (for a detailed description of this see Mortier et al. 2013b). Due to the fact that most of stars in our sample have temperatures lower than 5200 K, we adopt as final the parameters derived using the TS13 line-list. For the stars with temperatures greater than 5200 K, one still can adopt the results of the SO08 line-list. These stars are highlighted in Table 1. Please note that in the present analysis we use only the parameters derived using

[4] http://www.as.utexas.edu/chris/moog.html
[5] For a general review of the ARES+MOOG method used here see Sousa (2014).
[6] http://www.eso.org/observing/etc/bin/gen/form?INS.INS.NAME=UVES+INS.MODE=spectro

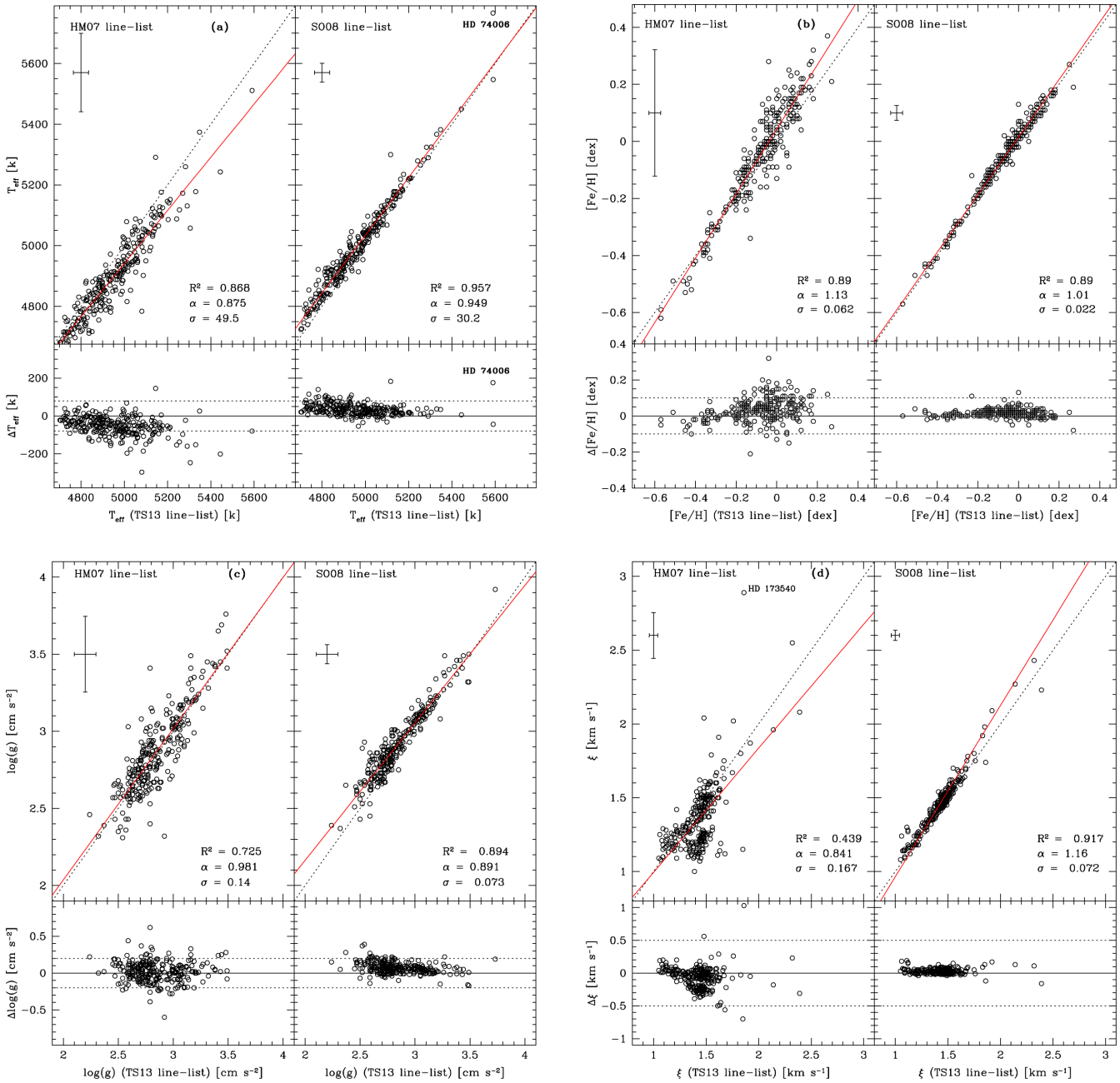

Figure 4. Comparison between the results found using the TS13, SO08, and HM07 line-lists. (a) Effective temperature, (b) metallicity, (c) surface gravity, and (d) microturbulence velocity derived using the HM07 (left-hand plot) and SO08 (right-hand plot) line-lists compared to those derived using the TS13 line-list. In each panel, the lower plot compares the differences from perfect agreement. The differences refer to the abscissa minus the ordinate of the corresponding upper plot. The dotted line shows the one-to-one relation, and the solid line is the linear fit, for which is given the values of the R-squared R^2, the slope calculated by the regression α, and the residual standard deviation σ. The average error is also plotted. HD 74006 is not shown in the plots presenting the results found using the HM07 line-list.

the TS13 line-list. In addition, particular attention should be taken when using the results presented in Table 1 concerning the possibility to round the numbers, especially for effective temperature and microturbulence. We have chosen not to round the numbers, but present them as they were delivered by the code.

In Fig. 2, we present he distribution of the atmospheric stellar parameters derived in our work, using, respectively, the HM07 (left-hand panel), SO08 (middle panel), and TS13 (right-hand panel) line-lists. We can see a general agreement for the results found for the three cases (HM07, SO08, and TS13 line-lists). The results from TS13 and SO08 are compatible in terms of metallicity, but in effective temperature they show an offset, specially for the cooler stars, as expected and discussed in TS13 and Mortier et al. (2013a). The uncertainties are illustrated in the boxplot in Fig. 3 which shows the median and quartiles for each parameters derived with the HM07 (left-hand panel), SO08 (middle panel), and TS13 (right-hand panel) line-lists. As we can see in this figure, HM07 results show a much higher dispersion on the uncertainties, as expected

Table 2. Stellar parameters of 74 stars common with our sample. References are provided into the table.

HD number	$T_{\rm eff}$ (K)	$\epsilon(T_{\rm eff})$	$\log g$ (cm s^{-2})	$\epsilon(\log g)$	[Fe/H] (dex)	ϵ([Fe/H])	ξ (km s^{-1})	$\epsilon(\xi)$	Ref.
496	4893	–	3	–	0.13	–	1.5	–	(1)
770	4696	100	2.68	0.1	−0.12	0.1	1.4	0.2	(2)
1737	5020	–	2.73	–	0.16	0.12	1.44	–	(3)
5457	4780	–	2.74	–	−0.07	0.14	1.38	–	(3)
8651	4708	100	2.67	0.1	−0.18	0.1	1.4	0.2	(2)
9362	4754	100	2.61	0.1	−0.28	0.1	1.3	0.2	(2)
10142	4688	100	2.65	0.1	−0.1	0.1	1.4	0.2	(2)
11977	4975	70	2.9	0.2	−0.14	0.05	1.6	–	(4)
12296	4860	–	2.71	–	−0.03	0.14	1.47	–	(3)
12438	4975	70	2.5	0.2	−0.54	0.05	1.5	–	(4)
16815	4732	100	2.6	0.1	−0.33	0.1	1.3	0.2	(2)
16975	5015	100	2.91	0.1	0.01	0.1	1.3	0.2	(2)
17652	4820	–	2.45	–	−0.37	0.08	1.42	–	(3)
23719	5070	–	2.85	–	0.11	0.11	1.43	–	(3)
23940	4910	–	2.63	–	−0.33	0.11	1.39	–	(3)
29085	4875	–	3.1	–	−0.2	–	1.35	–	(6)
29291	4960	–	2.92	–	−0.09	–	2.2	–	(7)
32436	4640	–	2.65	–	0.02	–	1.9	–	(7)
34266	5030	–	2.58	–	0.1	0.1	1.43	–	(3)
34642	4870	70	3.3	0.2	0.03	0.05	1.3	–	(4)
36189	5081	70	2.8	0.2	0.05	0.05	1.9	–	(4)
37811	5220	–	2.94	–	0.08	0.1	1.39	–	(3)
40409	4755	–	3.3	–	0.13	–	1.8	–	(8)
60666	4750	–	2.6	–	−0.02	–	1.38	–	(6)
67762	4980	–	3.26	–	−0.06	0.07	1.07	–	(3)
70982	5089	70	3	0.2	0.04	0.05	1.6	–	(4)
73898	5030	–	3.03	–	−0.49	–	2	–	(7)
74772	5210	–	2.5	–	−0.03	–	1.5	–	(9)
81169	4975	–	2.41	–	−0.09	–	2.1	–	(10)
93773	4985	70	3	0.2	0	0.05	1.5	–	(4)
94510	5100	–	3	–	0.1	–	1.1	–	(9)
100708	4890	–	2.75	–	−0.08	–	1.5	–	(9)
104704	4810	–	2.81	–	−0.15	0.08	1.2	–	(3)
115310	5060	–	2.63	–	0.04	0.09	1.39	–	(3)
118338	5180	–	3	–	0.12	0.08	1.37	–	(3)
119250	4860	–	2.53	–	−0.18	0.1	1.43	–	(3)
120457	4985	–	2.85	–	0.15	0.08	1.31	–	(3)
121853	4925	–	2.55	–	−0.32	0.09	1.44	–	(3)
123151	4960	–	2.62	–	−0.22	0.09	1.51	–	(3)
129462	5000	–	2.72	–	−0.03	0.1	1.41	–	(3)
135760	4850	–	3.06	–	0.2	0.13	1.19	–	(3)
136014	4869	70	2.7	0.2	−0.39	0.05	1.5	–	(4)
139521	4930	–	3.28	–	−0.34	–	2.7	–	(7)
140329	5010	–	3.14	–	0.01	0.09	1.09	–	(3)
143546	4977	100	2.84	0.1	−0.05	0.1	1.3	0.2	(2)
146686	4699	100	2.8	0.1	0.23	0.1	1.3	0.2	(2)
157515	4980	–	3.15	–	−0.17	0.08	1.15	–	(3)
165135	4760	–	2.72	–	−0.36	–	2.1	–	(7)
165634	4980	–	2.65	–	−0.05	–	1.73	–	(6)
168838	4950	–	2.73	–	0.09	0.09	1.44	–	(3)
169767	4720	100	2.71	0.1	−0.2	0.1	1.2	0.2	(2)
169916	4689	100	2.66	0.1	−0.06	0.1	1.2	0.2	(2)
174295	4893	70	2.8	0.2	−0.17	0.05	1.5	–	(4)
177389	5131	70	3.7	0.2	0.09	0.05	1.1	–	(4)
189005	5060	–	2.78	–	−0.38	–	2.7	–	(7)
189080	4720	–	2.51	–	−0.17	0.1	1.29	–	(3)
195569	4980	–	2.78	–	0.05	0.1	1.35	–	(3)
196171	4788	100	2.69	0.1	−0.13	0.1	1.5	0.2	(2)
198232	4923	70	2.8	0.2	0.1	0.05	1.5	–	(4)
199951	5310	–	3	–	−0.01	–	1.6	–	(9)
207229	4945	–	2.59	–	0.03	0.1	1.43	–	(3)
208737	4995	–	2.41	–	0.05	0.1	1.55	–	(3)

Table 2. – *continued*

HD number	$T_{\rm eff}$ (K)	$\epsilon(T_{\rm eff})$	$\log g$ (cm s^{-2})	$\epsilon(\log g)$	[Fe/H] (dex)	ϵ([Fe/H])	ξ (km s^{-1})	$\epsilon(\xi)$	Ref.
213009	4800	–	2	–	−0.2	–	1.3	–	(13)
215104	4737	100	2.62	0.1	−0.2	0.1	1.5	0.2	(2)
216763	4841	100	2.72	0.1	−0.21	0.1	1.4	0.2	(2)
220790	4850	–	2.67	–	−0.27	0.13	1.37	–	(3)
222433	4860	–	3.05	–	−0.3	–	2.1	–	(7)
166599	5005	50	2.6	0.25	−0.03	0.09	–	–	(11)
175219	4720	–	2.44	–	−0.32	–	–	–	(12)
24160	5010	–	–	–	–	–	–	–	(5)
94890	4802	–	–	–	–	–	–	–	(5)
96566	4901	–	–	–	–	–	–	–	(5)
116243	5181	–	–	–	–	–	–	–	(5)
134505	4990	–	–	–	–	–	–	–	(5)

References. (1) Gratton & Ortolani (1986); (2) Liu et al. (2007); (3) Jones et al. (2011); (4) da Silva et al. (2006); (5) di Benedetto (1998); (6) Hekker & Meléndez (2007); (7) McWilliam (1990); (8) Thorén et al. (2004); (9) Jones et al. (1992); (10) Luck (1991); (11) Randich et al. (1999); (12) Meléndez et al. (2008); (13) Foy (1981)

given their smaller number of lines. These relatively small number of lines (16 Fe I and 6 Fe II) decrease the statistical strength of the determined stellar parameters, increasing the internal dispersion, especially for Fe II. For instance, the metallicity derived using this line-list present high values for the errors, with an average of about 0.22 dex, and ϵ [Fe/H] > 1.0 dex for nine stars.

Fig. 4 shows the comparison between the results obtained using the HM07 and SO08 line-lists with those obtained using the TS13 line-list which we adopt as final parameters. As pointed out before, we adopt the TS13 results because this line-list was built specifically for stars with $T_{\rm eff} < 5200$ K. Even for some stars that have higher $T_{\rm eff}$, we still adopt the values derived using the TS13 line-list, since these results are in perfect agreement with those derived using SO08, within the errors. If the results of SO08 and TS13 were not in such a remarkable agreement, we would adopt the results obtained using SO08, since this is a better line-list for the hottest stars (more line hence better precision and lower error). Between the results of TS13 and HM07, we found an average difference (defined as TS13–HM07 results) of 54 K, −0.019 dex, 0.075 km s^{-1}, and −0.032 dex for effective temperature, surface gravity, microturbulence, and metallicity, while between the results of TS13 and SO08 the average differences (defined as TS13–SO08 results) are −35 K, −0.071 dex, −0.033 km s^{-1}, and −0.015 dex. Such good agreement between the results of SO08 and TS13 may be due to the good quality of the spectra, with both high resolution and high S/N, in which case the SO08 line-list is probably less affected by blended lines. Microturbulences compares very well with SO08 line-list, but the results found with HM07 line-list are slightly higher than the other values, but still within the error bar. As a matter of fact, microturbulence is the most affected parameter when the smaller line-list of HM07 was adopted. In the bottom right of Fig. 4, panel (d), we can see that a group of stars is separated from the others in the trend, and thus for these stars the HM07 microturbulence results differ significantly from those obtained with the TS13 line-list. We may explain those large discrepancies due to the small EW interval of Fe I lines measured using the HM07 line-list, which did not allow a consistent determination of the microturbulence. In addition, note that HD 173540 has an abnormal error, $\xi = 2.89 \pm 1.46$ km s^{-1}. If, instead, we use the empirical formula derived by HM07 based on their results, $\xi = 3.7 - 5.1 \times 10^{-4} T_{\rm eff}$, to estimate the microturbulence for this star, we get $\xi = 0.9 \pm 0.06$ km s^{-1}. Furthermore, a more reliable value ($\xi = 1.2 \pm 0.01$ km s^{-1}) was found applying the formula from Ramírez, Allende Prieto & Lambert (2013), $\xi = 1.163 + 7.808 \times 10^{-4}(T_{\rm eff} - 5800) - 0.494(\log g - 4.30) - 0.050$[Fe/H]. A more deeper and detailed discussion about these offsets are presented by Mortier et al. (2013b).

4 COMPARISON WITH PREVIOUS WORKS

The large majority of the giant stars studied in this paper do not have any previous metallicity estimate derived from high-resolution spectroscopy. In order to compare our results with previous ones, we used several works (Foy 1981, Gratton & Ortolani 1986; McWilliam 1990; Luck 1991; Jones et al. 1992, 2011; di Benedetto 1998; Randich et al. 1999; Thorén, Edvardsson & Gustafsson 2004; da Silva et al. 2006; HM07; Liu et al. 2007; Meléndez et al. 2008; Soubiran et al. 2010) to compile a list of literature data for a set of 74 stars in our sample. The literature values of the atmospheric parameters for these common samples are listed in Table 2. Note that only 67 of these stars have all four parameters already calculated in previous works (see the last rows of the Table 2), hence we are providing here new precise spectroscopic atmospheric parameters for an amount of 190 stars. Fig. 5 show the comparison between our results obtained for the TS13 line-list, with those presented in these earlier works. As we can see in the panels of this figure, our results present good agreement with those listed in the literature.

The atmospheric parameters taken from literature for the 74 stars presented in the Table 2 can also be found in the PASTEL catalogue (Soubiran et al. 2010) but not the microturbulence velocity. Compared to the PASTEL catalogue we found an average difference (defined as TS13 – literature data) of 108 K, −0.02 dex, and 0.03 dex for effective temperature, surface gravity, and metallicity, respectively.

The common sample presented in Table 2 is composed by values taken from 13 different works. In order to test our results against samples homogeneously characterized, we checked our results, separately, against those from Jones et al. (2011), Liu et al. (2007), McWilliam (1990), and da Silva et al. (2006) due to the significant number of stars in common with these works. Fig. 6 shows the comparison of our stellar parameters with those from these works. We found an average difference of 20 K, −0.17 dex, −0.032 km s^{-1}, and −0.072 dex, respectively, for effective temperature, surface

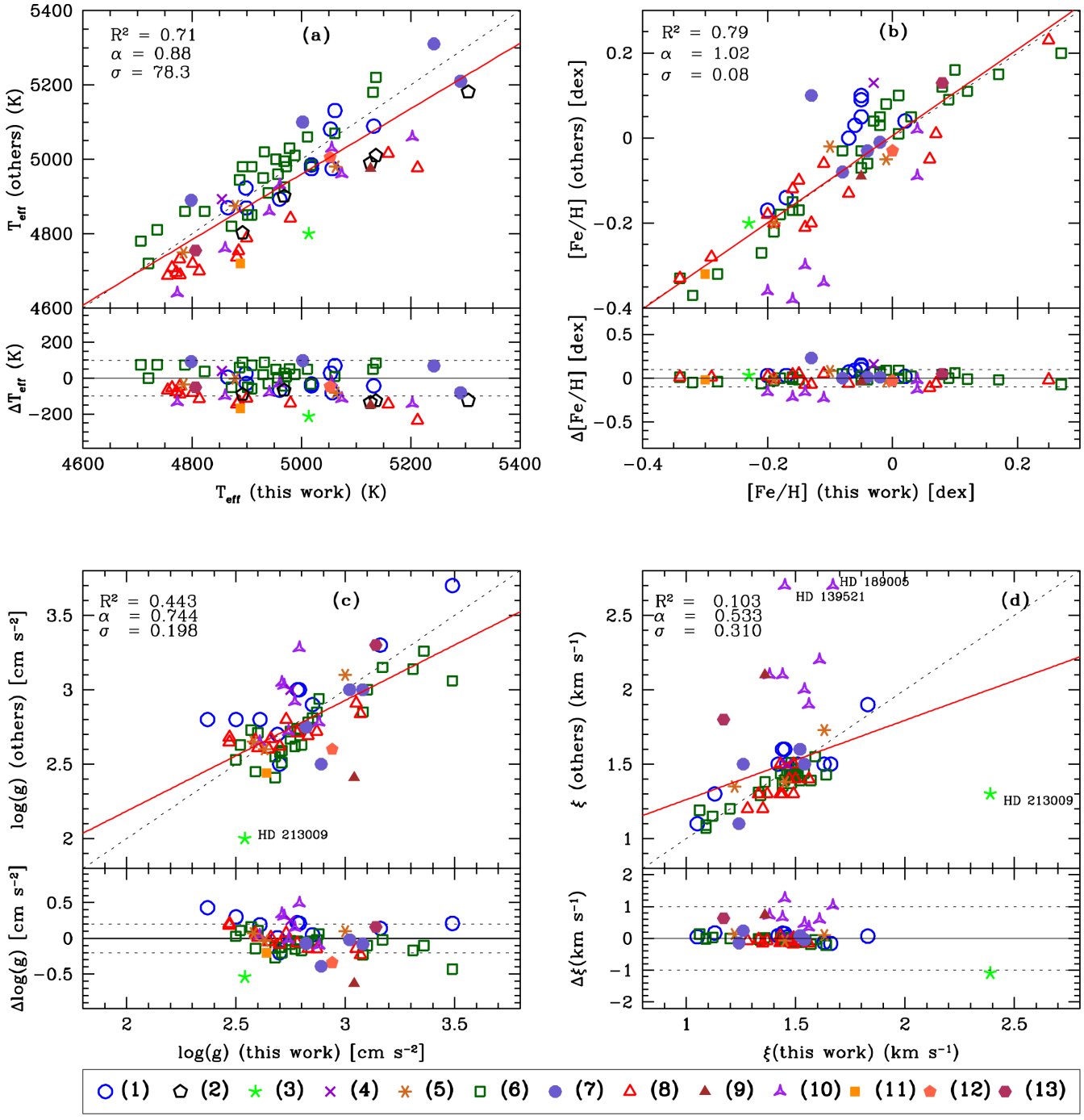

Figure 5. Comparison of the results of this work obtained for the TS13 line-list with available literature data for (a) effective temperature, (b) metallicity, (c) surface gravity, and (d) microturbulence. The dotted line shows the one-to-one relation, and the solid line is the linear fit, for which is given the values of the R-squared R^2, the slope calculated by the regression α, and the residual standard deviation σ. Each symbol indicates a reference given in Table 2, as enumeration given in the legend, i.e. (1): da Silva et al. (2006); (2): di Benedetto (1998); (3): Foy (1981); (4): Gratton & Ortolani (1986); (5): Hekker & Meléndez (2007); (6): Jones et al. (2011); (7): Jones et al. (1992); (8): Liu et al. (2007); (9): Luck (1991); (10): McWilliam (1990); (11): Meléndez et al. (2008); (12): Randich et al. (1999); (13): Thorén et al. (2004).

gravity, microturbulence, and metallicity when we compare our results with those from da Silva et al. (2006), and −26 K, 0.085 dex, 0.048 km s^{-1}, and −0.0088 dex compared to Jones et al. (2011).

We have 20 stars in common with McWilliam (1990), who analysed 671 GK giant spectra, and derived effective temperatures with empirical and semi-empirical methods, involving an IR flux calibration. For this set of stars, the average difference on effective temperature is 119 K, with a standard deviation of 81.1 K, and it is less than 0.12 dex in metallicity, with a standard deviation of 0.07 dex. Besides the effective temperature and the metallicity from McWilliam (1990) are marginally higher than the one derived in our work, the two other parameters compare quite well, with an average difference of −0.21 dex and −0.65 km s^{-1} for surface gravity and microturbulence, respectively.

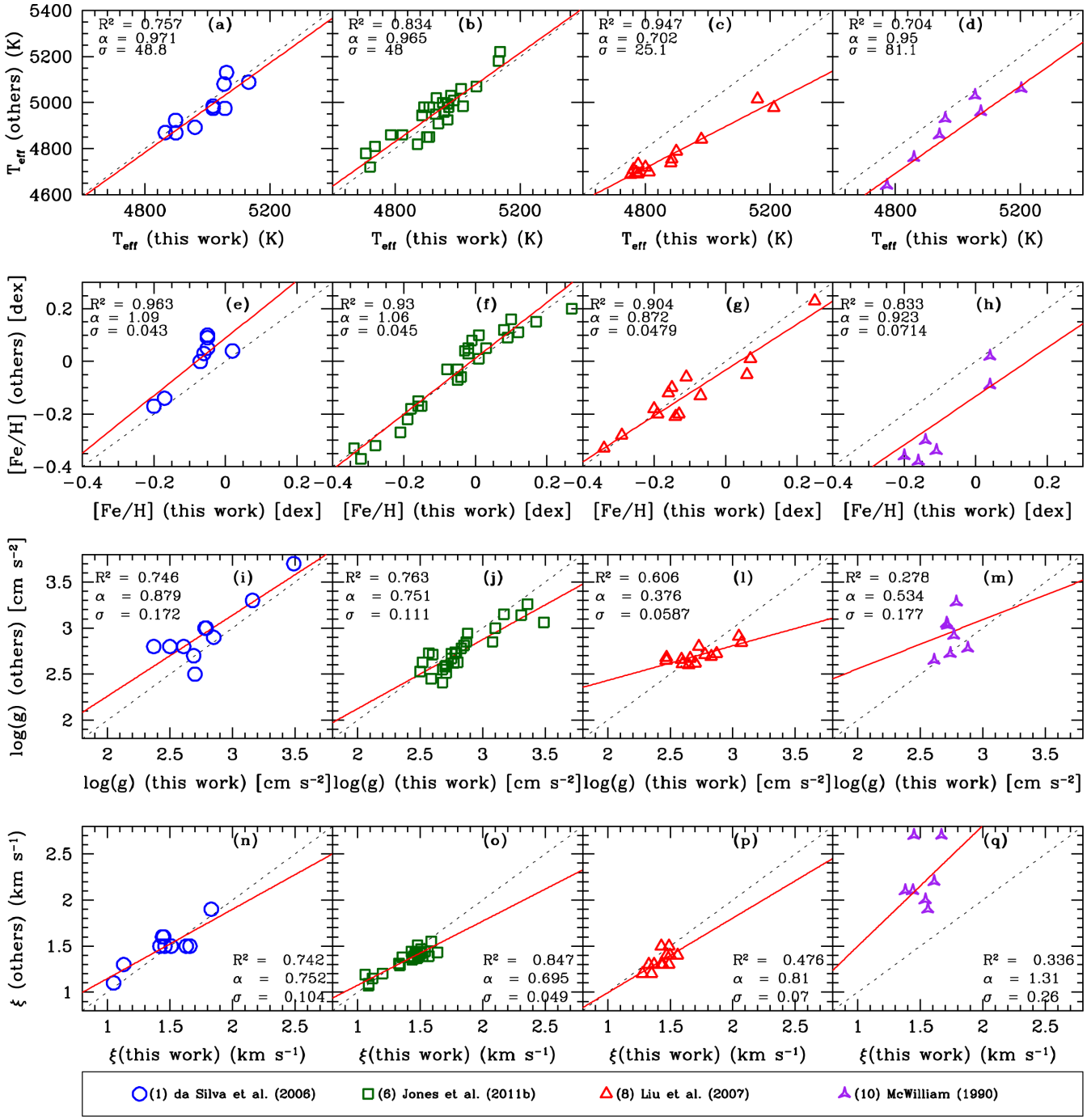

Figure 6. Comparison between our results with those from da Silva et al. (2006), Jones et al. (2011); Liu et al. (2007), and McWilliam (1990). The dotted line shows the one-to-one relation, and the solid line is the linear fit, for which is given the values of the *R*-squared R^2, the slope calculated by the regression α, and the residual standard deviation σ. Each symbol indicates a reference given in Table 2, as enumeration given in the legend.

The comparison of our atmospheric parameters with those from Liu et al. (2007), with whom we have 14 stars in common, is also presented in Fig. 6. The average differences are 108 K, 0.017 dex, 0.016 dex, and 0.089 km s^{-1}, respectively, for effective temperature, metallicity, surface gravity, and microturbulence.

5 CONCLUDING REMARKS

In this work, we have derived the stellar atmospheric parameters (the effective temperature, the surface gravity, the microturbulence, and the metallicity) for a sample of 257 field giant stars that are being surveyed for planets using precise radial-velocity measurements. Those parameters were derived by using three different line-lists of Fe I and Fe II (SO08, TS13, and HM07). All parameters derived in this work are listed in Table 1, and we adopt as final the parameters derived with the TS13 line-list. When one compares the results found by using the different line-lists we found small dispersion for most of the stars.

In the present catalogue (Table 1), we are providing new precise spectroscopic measurements of atmospheric parameters for

190 stars for which the given four parameters had not yet been found or published in previous articles. Additionally, we also provide new measurements for 67 stars with previous published results of all parameters, but with the major advantage that they are now calculated homogeneously, providing a more suitable analysis. The comparison of our results with those presented in the literature shows that our derivations are solid, and it will be very useful to future studies of frequency of planets as a function of the different stellar parameters, as a comparison sample.

Since the first discovery of a substellar companion orbiting a giant star (HD 137759 – Frink et al. 2002), more than 100 evolved stars are known to host planets according to the available data at the Extrasolar Planets Encyclopaedia,[7] but it is still missing a homogeneous sample that allows us to perform studies on the properties of giant stars hosting planets. Note that one star in our sample is already known to have an orbiting planet (HD 11977 – Setiawan et al. 2005). The parameters for this star are $T_{\rm eff} = 5018 \pm 27$ K, $\log g = 2.85 \pm 0.07$ cm s^{-2}, $\xi = 1.44 \pm 0.03$ km s^{-1}, [Fe/H] $= -0.17 \pm 0.03$ dex (TS13 line-list), showing that its metal content is a bit less than that of the Sun. Low metal abundance has been also found in other giants hosting planets suggesting that planet-hosting giant stars are on average metal-poor than planet-hosting dwarfs. However, as pointed out by Mortier et al. (2013a), it may be due to a bias in samples of evolved stars used to detect planets. For a more complete discussion of this subject the reader is directed to Mortier et al. (2013b) and Maldonado et al. (2013).

In the present catalogue, the red giant branch star HD 135760 is the most metal-rich ([Fe/H] $= +0.27 \pm 0.05$ dex), which is in agreement with previous result presented by Jones et al. (2011), while HD 7082 is the most metal-poor ([Fe/H] $= -0.74 \pm 0.02$ dex), amongst with three other stars that have [Fe/H] < -0.5 dex.

One of the major advantage of our work is to present a homogeneous calculation of spectroscopic parameters for a set of giant stars that have been already surveyed for planets, thus presenting a solid sample of comparison for future researches. Indeed, most stars of our sample have already a large number of measurements of precise radial velocities with the CORALIE spectrograph spread over the last years. Once a significant sample of planets is found in the present sample, we will be able to do analysis of the planet frequency as a function of metallicity and stellar mass. Until then, we can use our accurate and uniform stellar parameters as control sample to others studies that compares stars hosting planets with stars without detected planets. In addition, a complete study of chemical abundances for those stars (i.e. Table 1) will be released by Adibekyan et al. (in preparation).

ACKNOWLEDGEMENTS

This work was supported by the European Research Council/European Community under the FP7 through Starting Grant agreement number 239953. This work was also supported by the Gaia Research for European Astronomy Training (GREATITN) Marie Curie network, funded through the European Union Seventh Framework Programme ([FP7/2007-2013]) under grant agreement number 264895. NCS was supported by FCT through the Investigator FCT contract reference IF/00169/2012 and POPH/FSE (EC) by FEDER funding through the programme 'Programa Operacional de Factores de Competitividade' – COMPETE. VZhA and SGS are supported by grants SFRH/BPD/70574/2010 and SFRH/BPD/47611/2008 from the FCT (Portugal), respectively. Research activities of the Obsevational Stellar Board of the Federal University of Rio Grande do Norte are supported by continuous grants of CNPq and FAPERN brazilian agencies and by the INCT-INEspaço. SA acknowledges Post-Doctoral Fellowship from the CAPES brazilian agency (PNPD/2011: *Concessão Institucional*), Post-Doctoral Fellowship CAPES/PDE (BEX-2077140), and also support by Iniciativa Científica Milenio through grant IC120009, awarded to The Millennium Institute of Astrophysics. Authors are very thankful to referee, Chris Sneden, for his very constructive and helpful remarks that helped us to improve the paper.

[7] http://exoplanet.eu

REFERENCES

Boss A. P., 2002, ApJ, 567, L149
Cochran W. D., Endl M., Wittenmyer R. A., Bean J. L., 2007, ApJ, 665, 1407
da Silva L. et al., 2006, A&A, 458, 609
di Benedetto G. P., 1998, A&A, 339, 858
Ekström S. et al., 2012, A&A, 537, A146
Fischer D. A., Valenti J., 2005, ApJ, 622, 1102
Flower P. J., 1996, ApJ, 469, 355
Foy R., 1981, A&A, 93, 315
Frink S., Mitchell D. S., Quirrenbach A., Fischer D. A., Marcy G. W., Butler R. P., 2002, ApJ, 576, 478
Ghezzi L., Cunha K., Schuler S. C., Smith V. V., 2010, ApJ, 725, 721
Gratton R. G., Ortolani S., 1986, A&A, 169, 201
Hekker S., Meléndez J., 2007, A&A, 475, 1003 (HM07)
Ida S., Lin D. N. C., 2004, ApJ, 616, 567
Jones K. L., Robinson R. D., Slee O. B., Stewart R. T., 1992, MNRAS, 256, 535
Jones M. I., Jenkins J. S., Rojo P., Melo C. H. F., 2011, A&A, 536, A71
Kennedy G. M., Kenyon S. J., 2008, ApJ, 673, 502
Kurucz R., 1993, ATLAS9 Stellar Atmosphere Programs and 2 km/s grid. Kurucz CD-ROM No. 13. Smithsonian Astrophysical Observatory, Cambridge, Mass
Liu Y. J., Zhao G., Shi J. R., Pietrzyński G., Gieren W., 2007, MNRAS, 382, 553
Lloyd J. P., 2013, ApJ, 774, L2
Luck R. E., 1991, ApJS, 75, 579
McWilliam A., 1990, ApJS, 74, 1075
Maldonado J., Villaver E., Eiroa C., 2013, A&A, 554, A84
Meléndez J. et al., 2008, A&A, 484, L21
Mordasini C., Alibert Y., Klahr H., Henning T., 2012, A&A, 547, A111
Mortier A., Santos N. C., Sousa S., Israelian G., Mayor M., Udry S., 2013a, A&A, 551, A112
Mortier A., Santos N. C., Sousa S. G., Adibekyan V. Z., Delgado Mena E., Tsantaki M., Israelian G., Mayor M., 2013b, A&A, 557, A70
Pasquini L., Döllinger M. P., Weiss A., Girardi L., Chavero C., Hatzes A. P., da Silva L., Setiawan J., 2007, A&A, 473, 979
Perryman M. A. C. et al., 1997, A&A, 323, L49
Ramírez I., Allende Prieto C., Lambert D. L., 2013, ApJ, 764, 78
Randich S., Gratton R., Pallavicini R., Pasquini L., Carretta E., 1999, A&A, 348, 487
Reffert S., Bergmann C., Quirrenbach A., Trifonov T., Künstler A., 2015, A&A, 574, 116
Santos N. C., Israelian G., Mayor M., 2004, A&A, 415, 1153
Santos N. C., Melo C., James D. J., Gameiro J. F., Bouvier J., Gomes J. I., 2008a, A&A, 480, 889
Santos N. C. et al., 2008b, A&A, 487, 369
Santos N. C., Lovis C., Pace G., Melendez J., Naef D., 2009, A&A, 493, 309
Setiawan J. et al., 2005, A&A, 437, L31
Sneden C. A., 1973, PhD thesis, Univ. Texas at Austin

Soubiran C., Le Campion J.-F., Cayrel de Strobel G., Caillo A., 2010, A&A, 515, A111
Sousa S., 2014, in Niemczura E., Smalley B., Pych W., eds, Determination of Atmospheric Parameters of B-, A-, F- and G-Type Stars, GeoPlanet: Earth and Planetary Sciences. Springer International Publishing, p. 297
Sousa S. G., Santos N. C., Israelian G., Mayor M., Monteiro M. J. P. F. G., 2007, A&A, 469, 783
Sousa S. G. et al., 2008, A&A, 487, 373 (SO08)
Sousa S. G., Santos N. C., Israelian G., Mayor M., Udry S., 2011, A&A, 533, A141
Thorén P., Edvardsson B., Gustafsson B., 2004, A&A, 425, 187
Torres G., 2010, AJ, 140, 1158
Tsantaki M., Sousa S. G., Adibekyan V. Z., Santos N. C., Mortier A., Israelian G., 2013, A&A, 555, A150 (TS13)
Udry S. et al., 2000, A&A, 356, 590

This paper has been typeset from a TEX/LATEX file prepared by the author.